Molecular dynamics simulations of the interactions of DMSO, mono- and polyhydroxylated cryosolvents with a hydrated phospholipid bilayer.

Chris J. Malajczuk[a], Zak E. Hughes[a,1], and Ricardo L. Mancera[a*]

[a]*Western Australian Biomedical Research Institute, Curtin Health Innovation Research Institute, School of Biomedical Sciences, Curtin University, P.O. Box U1987, Perth WA 6845, Australia.*

Abstract

Molecular dynamics (MD) simulations have been used to investigate the interactions of a variety of hydroxylated cryosolvents (glycerol, propylene glycol and ethylene glycol), methanol and dimethyl sulfoxide (DMSO) in aqueous solution with a 1,2-dipalmitoyl-sn-glycero-3-phosphatidylcholine (DPPC) bilayer in its fluid phase at 323 K. Each cryosolvent induced lateral expansion of the membrane leading to thinning of the bilayer and resulting in disordering of the lipid hydrocarbon chains. Propylene glycol and DMSO were observed to exhibit a greater disordering effect on the structure of the membrane than the other three alcohols. Closer examination exposed a number of effects on the lipid bilayer as a function of the molecular size and hydrogen bonding capacity of the cryosolvents. Analyses of hydrogen bonds revealed that increased concentrations of the polyhydroxylated cryosolvents induced the formation of a cross-linked cryosolvent layer across the surface of the membrane bilayer. This effect was most pronounced for glycerol at sufficiently high concentrations, which displayed a comparatively enhanced capacity to induce cross-linking of lipid head groups

[1] Present address: Institute for Frontier Materials, Deakin University, Waurn Ponds, VIC 3216, Australia.

* Corresponding author: School of Biomedical Sciences, Curtin University, P.O. Box U1987, Perth WA 6845, Australia. Tel: +618 9266 1017; fax: +618 9266 2342.
E-mail address: R.Mancera@curtin.edu.au (R.L. Mancera).

resulting in the formation of extensive hydrogen bonding bridges and the promotion of a dense cryosolvent layer across the phospholipid bilayer.

Keywords: methanol; propylene glycol; ethylene glycol; glycerol; DPPC; molecular dynamics

1. Introduction

Cryopreservation is a viable option for the long-term storage of vegetatively propagated species and such techniques have been developed and applied to upwards of 100 plant species world-wide [1, 2]. Cryopreservation of flora entails the conservation of plant propagules by storage at liquid nitrogen temperatures (77 K) such that the natural metabolic processes are suspended [1-3]. The process of rapid-cooling of biological solutions *via* cryopreservation techniques allows for relatively normal cellular integrity and function to be maintained by promoting the formation of a "glassy" or vitrified state below normal freezing temperatures [4, 5]. However, in practice the process of supercooling can cause damage to cells through the formation of intra- and extracellular ice, cell desiccation and phase changes of the cell membranes [1-5]. The addition of cosolutes known as cryosolvents to solutions promotes the transition of liquid water to an amorphous solid (vitrified) state at a higher temperature upon rapid cooling [4, 5], commonly believed to be a result of the ability of cryosolvents to increase the viscosity of water such that the nucleation of water is inhibited [4-8].

Vitrification in cryopreserved tissues helps to prevent the formation of extracellular ice, which would otherwise lead to an increase in the extracellular electrolyte concentration, resulting in the redistribution of water from within the cell to its surrounds *via* osmosis [9, 10]. Severe efflux of this kind can result in cellular dehydration and shrinkage, leading to the intracellular solutes becoming more concentrated and potentially increasing the rate of destructive chemical reactions [11]. Cell shrinkage, which occurs as a result of the external

osmotic pressure, creates suction of the intracellular aqueous phase, which opposes natural intramembrane repulsion between phospholipids (the major components of cell membranes) to bring membranes closer together. The elasticity of the cell membrane acts to resist this unfavourable cell shrinkage caused by compressive lateral stresses by stretching the phospholipid acyl tails vertically resulting in a thickened and more ordered membrane [9]. Whilst the resulting thickened lipid plane is not understood to result in irreversible ultrastructural membrane deformation per se, the resulting anisotropic structural stresses can induce strains that cause changes to the membrane fluidity (liquid-gel transition) or cause component separation of the cell membrane to produce the irreversible inverse hexagonal-II phase transition in domains of weakly hydrating lipid components [9, 12].

In contrast to liquid-crystal phase bilayers, the lipids in a gel phase bilayer have limited lateral and flip-flop mobility, which hinders the ability of a cell to reseal membrane tears [11]. Cells subject to freezing temperatures have a greater propensity to suffer structural faults [13] and an inability of the membrane to repair such damage can lead to cell elution and thus cell death [13, 14]. In addition to the fluid-gel phase transitions, fluid-fluid demixing resulting from compressive lateral stresses can lead to membrane reshuffling, leading to the aggregation of large-hydrating components such as intrinsic membrane proteins [15]. As a response to compressive stresses in the interfacial plane of the membrane, the resulting low-hydrating domains of lipids adjust to relax the strain by undergoing inverse hexagonal-II phase transitions [10]. This phase transition involves lipid headgroups rearranging to surround small, cylindrical water cores on a two dimensional hexagonal lattice [10, 15] and has been shown to cause irreversible damage to the cell membrane by compromising the essential semi-permeable nature of lipid membranes [10, 14]. Such cell deformation resulting from desiccation is recognised as being one of the major factors hindering the survival of cryopreserved tissues [16].

The integrity of the cell membrane is thus critical in preventing cell death as a consequence of freezing damage. The cell membrane aids in the prevention of extracellular ice extending to the interior of the cell by acting as a physical barrier, whilst also maintaining the different concentrations and compositions of intra- and extracellular solutions by providing hydraulic permeability [5, 10]. In order to maintain the structural integrity of cell membranes by avoiding intracellular ice formation and deleterious phase transitions at freezing temperatures, it has been shown that the combination of supercooling, depression of the equilibrium freezing point, dehydration and intracellular vitrification must be achieved [5]. Accumulation of cryosolvents at sufficiently high concentrations within the cellular medium has been shown to promote the vitrification of water and also modulate the properties of the cell membrane to aid these processes [10].

Dimethyl sulfoxide (DMSO) is the most commonly used cryosolvent due to its ability to reduce ice formation in biological solutions [7] through its capacity to promote the vitrification of water [4, 5]. Due to its dual hydrophilic and hydrophobic nature [17-19], DMSO is highly soluble in water and can also readily diffuse across a lipid bilayer [20], and at appropriate concentrations can partition within an intermembrane space to limit membrane compression by forming a physical barrier between lipid headgroups [10]. DMSO is, however, toxic to cells and minimisation of the exposure time and/or the concentration of DMSO is a common strategy for the optimisation of cryoprotection protocols [21]. Atomic-scale molecular dynamics (MD) simulations have provided insight into the molecular mechanism of interaction of DMSO with phosphocholine bilayers in the liquid-crystalline phase [22-29], describing three distinct, concentration-dependent modes of action: at low concentrations DMSO induces membrane thinning and thus increases membrane fluidity, at higher concentrations the formation of pores across the bilayer is observed, and at even higher concentrations constituent lipids are desorbed from the membrane leading to

membrane disintegration [23]. The presence of sterols in these phosphocoline bilayers reduces these deleterious effects [30].

Polyhydroxylated solvents such as propylene glycol (PG), ethylene glycol (EG) and glycerol (GLY) (see Fig. 1) are common substitutes for DMSO as cryoprotectants as they exhibit lower toxicity at relative concentrations [31, 32], have an ability to broaden the glass transition state of water and modulate the properties of cell membranes [33-36]. Differential scanning calorimetry (DSC) measurements of the interaction of PG with a membrane bilayer have suggested that it has the ability to enhance bilayer penetration by increasing membrane fluidity [37]. It has also been suggested that EG and GLY act to stabilise the liquid-crystalline phase of phospholipid bilayers through partitioning behaviour to also increase membrane fluidity [34, 38, 39]. At sufficiently high concentrations methanol (MET), although toxic, has been shown to behave in a similar fashion to these polyhydroxylated solvents by enhancing the fluidity of membrane bilayers [34, 40-42]. The toxicity of each of these hydroxylated compounds is concentration dependent, with GLY and EG being less harmful to cell survival than PG and DMSO at equivalent concentrations [12, 13]. Both DMSO and the alcohols have been shown experimentally [43-48] to induce lipid phase changes from the liquid-crystalline phase to the gel phase at sufficiently high concentrations (10 mol. % DMSO increases such a lipid phase transition of a DPPC membrane from 314.4 K to 320 K [49]).

One prior MD study has reported investigating PG in the presence of a pure phospholipid bilayer, describing a strong disordering effect on the 1,2-dioleoyl-sn-glycero-3-phosphocholine (DOPC) bilayer as concentration of PG increases, demonstrating an action comparable to DMSO [50]. PG was reported to exhibit a high affinity for the pure DOPC bilayer, intercalating between phospholipid headgroups leading to significant membrane thinning and lateral expansion comparative to MET, EG and GLY at the same concentrations [50]. At sufficiently high concentrations (25.0 mol. %), PG was shown to induce membrane pore formation whilst the surrounding DOPC bilayer mostly retained its structural stability

[50]. As in the case of DMSO [30], addition of β-sitosterol reduced the damaging effect of these cryosolvents [50].

Only a few MD simulation studies have characterised bilayer systems in the presence of GLY, EG and MET [7, 34, 40, 50-52]. With the exception of the work of Pereira *et al.* with GLY [34], the previous MD simulations of pure 1,2-dipalmitoyl-*sn*-glycero-3-phosphatidylcholine (DPPC) bilayers in the presence of GLY, EG and MET were in good qualitative agreement with experimental studies, describing membrane lateral expansion and thinning normal to the plane of the bilayer when in the presence of each cryosolvent, leading to increased disorder in the hydrocarbon acyl tail groups of the phospholipids. Pereira *et al.* found that GLY (at a concentration of 10.3 mol. %) was essentially inert with respect to the DPPC bilayer leading to no noticeable change in membrane structure [34]. The same study described EG (at a concentration of 8.5 mol. %) to preferentially aggregate at the phosphate headgroups of phospholipids [34]. Contrastingly, Kyrychenko *et al.* reported that GLY (at a concentration of 6.2 mol. %) preferentially aggregated at the phospholipid headgroups, whilst EG (at a concentration of 13.3 mol. %) was shown to exhibit preferential affinity to the phospholipid glycerol groups towards the bilayer interior [7]. MET was the only alcohol reported to consistently penetrate the phospholipid membrane and partition between headgroups across various concentrations (1 mol. % up to 25 mol. % [29, 34, 40, 50, 51]); however, the disparity in simulation conditions and specific concentrations of MET in the presence of a lipid bilayer in these MD studies underpins the need for further investigation to clarify and characterise the specific mode of action of MET. We have thus conducted a series of MD simulations of the interactions of these hydroxylated cryosolvents with a DPPC bilayer to try to develop a consensus of their molecular mechanism of action across a range of concentrations.

2. System

2.1. Model and simulation details

Fully hydrated DPPC bilayer systems were constructed consisting of 128 lipid molecules (64 DPPC lipids in each leaflet) in the presence of 5841 solvent molecules, and all MD simulations were performed using GROMACS v.3.3.3 [53]. Phospholipids were modelled using the GROMOS 53A6L [54, 55] force-field (which forms part of the GROMOS 54A7 parameter set [56]), water molecules were described by the SPC potential [57] and the cryosolvents MET, EG, GLY, PG and DMSO were represented by a united-atom model that forms part of the standard GROMOS 53A6 and 54A7 force-fields [56, 58]. The initial membrane configurations were taken from pre-equilibrated DPPC membranes solvated in water at a temperature of 323 K [59]. The total number of solvent molecules in the system was kept constant at 5841 and with each cryosolvent added to the system replacing one water molecule. The DPPC bilayers were simulated in solutions of cryosolvents at concentrations of 2.5, 5.0, 10.0, 15.0 mol. %, corresponding to solutions containing 146, 292, 584 and 876 cryosolvent molecules, respectively. A DPPC bilayer solvated in 15.0 mol. % DMSO was not simulated due to the fact that at 323 K 15.0 mol. % DMSO will induce a phase transition to the gel phase for a DPPC membrane [60]. The cryosolvent concentrations were chosen to provide a realistic range for the investigation of concentration-dependent regimes associated to each cryosolvent, whilst consistency of concentration across all DPPC-cryosolvent systems allows for comparison between the effects of the cryosolvents at equivalent concentrations. In addition, to provide a comparison with previous work, a DPPC system containing 25.0 mol. % MET was also simulated, and two additional intermediate concentrations of GLY at 7.5 and 12.5 mol. % were simulated to clarify observed behavioural trends unique to this alcohol. The bilayers lie in the *xy* plane with the bilayer normal parallel to the *z*-axis.

The lipid and solvent molecules were weakly coupled separately to a temperature bath at 323K using the Berendsen thermostat [61] with a coupling time constant of 0.1 ps, and the bath temperature for all simulations was maintained at this temperature. Pressure was

maintained at 1 bar such that the *x*/*y*- and *z*-axes of the simulation box were independently coupled to a Berendsen barostat [61] with a time constant of 1.0 ps. Accordingly, the height of the simulation box and the cross sectional area were allowed to vary independently of each other, thereby allowing the surface area of the bilayer and the distance between the interfaces to fluctuate independently.

The non-bonded Lennard-Jones interactions were calculated using a twin-range cut-off: interactions at a distance within 0.8 nm were calculated every step and interactions within 1.4 nm were updated every five time steps along with the pair list. Long-range electrostatic interactions were computed using a reaction-field correction where the relative dielectric permittivity constant (εRF = 62) was appropriate for SPC water. The equations of motion were integrated using the leap-frog algorithm [62] with a time step of 2.0 fs. All systems were simulated for a total of 200 ns, with the final 60 ns of the simulations used for analysis. The atomic coordinates and velocities were saved every 2 ps for analysis.

2.2. Data analysis

The area per lipid (APL) describes the average area occupied by each individual lipid at a given frame in a simulation, and was calculated *via* the Voronoi analysis [63]. The standard deviation of APL measurements was calculated for each system and factored into the final APL result as the statistical error.

The average mass density profile (MDP) across the bilayer was determined by separately analysing each frame across the equilibrated sample set. Computation of the centres of mass for the two lipid monolayers allows for determination of the centre of the bilayer (ie. the *z* component), and the positions of all atoms of interest were taken into account with respect to this centre [64]. The thickness of the bilayer was calculated as the distance between the average peak heights of phosphate MDPs for each system. Bulk-to-peak height ratios were

calculated from the trough and peak number density values for each cryosolvent in a given system.

Radial distribution functions (RDF) between choline and glycerol groups of the phospholipids and water molecules were calculated individually [64] between water and the nitrogen and carbonyl oxygen groups of choline and glycerol respectively. The first solvation shell was defined as the point of the first local minimum in the resulting RDFs found: 0.64 and 0.32 nm for the choline and the glycerol groups, respectively. The coordination numbers of water molecules to the lipid groups are defined as the average number of water molecules found in the first solvation shells. The deuterium order parameter, SCD, describes the relative orientation of carbon-deuterium (C-D) bonds of the phospholipid hydrocarbon tail groups with respect to the bilayer normal and is calculated from

$$S_{CD} = ½ (3cos^2 \theta - 1) \quad (1)$$

where θ is the angle between a C-D of a methylene group in the hydrocarbon chain and the bilayer normal [22, 64]. As the lipid model used is an united-atom model the deuterium atom position is determined from the position of neighbouring carbons in the hydrocarbon chains and assuming a tetrahedral geometry of the methylenes [22, 64].

Hydrogen bonding of cryosolvents and water molecules to the DPPC phosphate and glycerol groups was defined as a hydrogen-acceptor distance shorter than 0.35 nm and a hydrogen-donor-acceptor angle with a cut-off of 30˚ [34]. All the oxygen atoms of the phosphate and glycerol groups of DPPC lipids were considered as hydrogen-bond acceptors, and all the hydroxyl groups of cryosolvents were considered as hydrogen-bond donors and acceptors.

The hydrogen bonding affinity (HBA) was defined as the average number of hydrogen bonds per molecule, and where indicated was normalised for the total number of hydrogen bond donor and acceptor groups in each molecule.

3. Results and Discussion

Monitoring the time evolution of the area per lipid (APL) of membrane systems is recognised as an appropriate proxy for system equilibration. It was observed that, in the absence of cryosolvents, the APL of the DPPC bilayer was 0.622 ± 0.009 nm^2, a result very close to the published experimental value for DPPC in the liquid crystalline phase at 323 K (0.628 nm^2) [65], and well within the range of reported experimental values for DPPC under these conditions (0.57 – 0.717 nm^2) [55]. Addition of cryosolvents into the DPPC bilayer system led to an initial rapid increase in APL for approximately the first 10-25 ns, before increasing steadily to a new, adjusted equilibrated state (see Fig. 2). The initial increase is likely to reflect the favourable driving force associated with the replacement of water molecules at the bilayer surface by cryosolvent molecules, leading to interaction and aggregation at the membrane interface as opposed to remaining in the bulk solution [34, 51, 52]. The subsequent steady increase reflects the gradual equilibration of each system, further enhancing the affinity of the cryosolvents for the membrane. This equilibration period was measured to last up to 100 ns (15.0 mol. % GLY). The required length of equilibration time of these systems and their propensity to fluctuate as a consequence of statistical variation highlights the necessity to run these simulations for an extended period of time.

The average APL and membrane thickness trends observed for a DPPC bilayer in the presence of each cryosolvent are summarised in Table 1. It can be seen that addition of all the species induces an increase in APL across the investigated concentrations due to the lateral expansion of the bilayer. This trend is complemented by a decrease in membrane thickness normal to the plane of the bilayer, $d_{membrane}$, in all bilayer systems in the presence of the alcohols. These observations suggest that lateral expansion and thinning of the bilayer is

induced by the addition of each cryosolvent, which is in good qualitative agreement with experimental observations for the alcohols [35-39, 42].

The effect of changing the concentration of cryosolvents on the APL of the DPPC bilayer is illustrated in Fig. 3. It is apparent that the different cryosolvents appear to fall into two groups based on considerable overlap between the APL trend lines: PG and DMSO form one group and the remaining three alcohols, MET, EG and GLY, form the other. Addition of PG and DMSO is observed to induce lateral expansion of the membrane which is higher than for MET, EG and GLY, consistent with our recent report of the effect of these cryosolvents on DOPC membranes at 350 K [50]. It should be noted that DMSO concentrations of 10.0 mol. % are reported to cause the bilayer to undergo a phase transition to the lipid gel phase at 320K [49], hence the APL results beyond 10.0 mol. % DMSO are not included. The trends observed in Table 1 for the membrane thickness complement the APL findings, indicating that PG has a greater ability to thin a DPPC membrane than the other three hydroxylated compounds at equivalent concentrations. Under the same conditions, DPPC bilayers in the presence of DMSO at concentrations of 10.0 mol. % are observed to undergo relatively pronounced distortion, resulting in decreased regularity across the bilayer surface. As a consequence, an increase in the average membrane thickness for DPPC bilayers in the presence of DMSO is observed between 5.0 and 10.0 mol. %, though this value is suitably compromised by its standard error (see Fig. 4).

Exact comparisons of APL predictions in previous MD studies cannot be made due to dissimilar system conditions; however, associations can be inferred based on their relative concentrations. Earlier studies described a greater influence of MET on the APL at lower concentrations (6 % increase at ~1.0 mol. %) [29, 40], but a less pronounced effect at increasing concentrations (15% increase at 11.3 mol. %, and 27% increase at 23.5 mol. %) [34, 51]. Previous MD simulations of DPPC bilayers in the presence of EG and GLY within the analysed concentration range indicated comparatively marginal APL increases to those

observed here, with predictions of 7% and 2% increase in APL for 13.3 mol. % EG and 10.3 mol. % GLY [7, 34], respectively, whilst at concentrations below 10.0 mol. % both cryosolvents produced up to a 3.1% increase in APL at concentrations of 8.5 mol. % and 6.2 mol. % for EG and GLY, respectively [7, 34]. MD simulations of a DPPC bilayer in the presence of DMSO at 325 K showed an ~11% increase in the APL for 5.00 mol. % DMSO [29] and coarse grained simulations running beyond 240 ns at 323 K have indicated that APL increases are observed for all investigated concentrations of DMSO up to 27.0 mol. % [27].

It is possible that the shorter simulation times of previous MD studies contribute to the observed discrepancies, with Kyrchenko *et al.* conceding that the total simulation time of 15 ns for their investigation was not sufficient for adequate MD sampling [7], whilst Pereira *et al.* allowed only 9 ns for equilibration for rather short 15 ns simulations, and Pinisetty *et al.* and Patra *et al.* defined ~15 ns and 20 ns equilibration times respectively for 50 ns simulations. However, it must be reiterated that the systems described in previous reports are distinct (as a consequence of using different force-field parameter sets, concentration regimes and simulation times) from those studied here and quantitative discrepancies are thus to be expected. Qualitatively, however, the action of each alcohol is consistent with these MD studies, whereby addition of each cryosolvent to a DPPC bilayer system led to membrane lateral expansion and thinning in the plane normal to the bilayer.

The mass density profile (MDP) perpendicular to the plane of a DPPC membrane describes the time averaged mass densities of cryosolvents, water and phospholipids across the bilayer normal, from which it is possible to obtain information about the structural stability of the lipid bilayer and the diffusional profile of water and cryosolvents across the membrane [7, 23, 34]. The MDPs of a DPPC bilayer in solutions of PG at different concentrations are illustrated in Fig. 5 (*A-D*), with the constituent phosphate groups of the bilayer included as a point of reference. At low concentration of PG (2.5 mol. %), it is evident that there is minimal structural disordering of the membrane as the characteristic DPPC bilayer profile is

largely retained. As concentration is increased to 10.0 and 15.0 mol. % the structural disordering of the membrane bilayer becomes increasingly evident, as characterised by widened phosphate profiles and a flattening of the DPPC profile. A thinning of the membrane is also observed between MDPs, which is consistent with the calculated APL and membrane thickness measurements. At these concentrations the greatest concentration of PG is to be found just above the position of the phosphate headgroups, suggesting that PG has a greater aggregating tendency at this region and could be the result of PG saturation at the lipid ester regions.

The MDPs shown in Fig. 6 suggest that all cryosolvents at 10.0 mol. % aggregate preferentially towards the lipid/water interface of the bilayer, and this result is consistent across all investigated concentrations of cryosolvents. DPPC bilayers in the presence of MET, EG, GLY and DMSO are noted to retain some structural ordering at this concentration, as evidenced by the characteristic peaks at the lipid/water interfaces (representative of phospholipid headgroups) and the trough towards the bilayer interior (representative of the hydrocarbon tail groups). PG (and DMSO) is also noted to exhibit a greater preferential aggregating tendency for the interior of the bilayer immediately past the phosphate groups than for the lipid/water interface. At concentrations of 15.0 mol. % for the three alcohols (results shown in the Supporting Information), this characteristic profile for DPPC is slightly diminished, but still prevalent. On the other hand, in the presence of 10.0 mol. % PG, the relative structural ordering of the DPPC bilayer appears to have been substantially compromised, as illustrated by a comparatively level profile. Unlike the hydroxylated cryosolvents, evidence of DMSO and water penetration through the bilayer at 10.0 mol. % is illustrated by non-zero DMSO and water profiles at the bilayer centre.

As a comparison to the action of PG on a DPPC bilayer at high concentrations, Fig. 6, *E* and *F* illustrates that high concentrations of GLY largely retain the characteristic peaks and

troughs of the DPPC profile, indicating that structural ordering of the bilayer is relatively less compromised compared with PG.

The number density profile for each cryosolvent in Fig. 7 illustrates the comparative preferential affinity of each alcohol to the bilayer for the tested concentrations. It is observed that at lower concentrations (2.5 and 5.0 mol. %), GLY displays a stronger tendency to aggregate preferentially at the external region of the bilayer than PG, EG, MET and DMSO, in that order respectively. At these concentrations PG, MET and DMSO are shown to also aggregate towards the region immediately below the phosphate groups of the bilayer, indicated by two distinguishable peaks at either side of the DPPC bilayer. Such behaviour is consistent with prior MD simulations of MET and DMSO at this concentration range [22, 23, 40, 50], and is a likely consequence of PG, MET and DMSO having a greater hydrophobic character relative to EG and GLY, allowing for increased penetration towards the hydrocarbon lipid chains [23]. At higher concentrations of cryosolvents (10.0-15.0 mol. %), EG and GLY appear to retain a strong, analogous aggregating tendency to the outer surface regions of the bilayer, whilst MET and PG preserve some affinity for the interior groups of the phospholipids but largely share this preference for the lipid/water interface. As concentration of the alcohols increases, the central hydrophobic region of the bilayer becomes increasingly infiltrated by cryosolvent molecules, with PG and MET exhibiting a greater capacity to permeate into this region than GLY and EG. Across all concentrations the centre of the bilayer remains nonetheless predominantly free from alcohol molecules. DMSO by contrast is observed to permeate much further, and in greater quantities, towards the interior of the membrane bilayer at 10.0 mol. % compared to the alcohols, such that a cryosolvent-free zone at the centre of the bilayer cannot be detected.

The aggregating tendency of each alcohol to the lipid bilayer is illustrated in Fig. 8, *A-D*, mirroring the density profile results. At concentrations of 2.5 mol. % there is a noticeable layer of GLY molecules across the bilayer surface relative to the other cryosolvents. The

cryosolvent bulk-to-peak height ratios in Table 2 are related to the tendency of each cryosolvent to be found aggregating at the bilayer interface region as opposed to being in the bulk solution. Across all concentrations it is evident that GLY exhibits the strongest tendency to aggregate at the lipid/water interface, with PG, EG, DMSO and MET exhibiting a lower aggregating tendency to the bilayer, in that order respectively. For the alcohols analysed, the aggregation tendency trends of these alcohols with the DPPC bilayer appear to be related to molecular size and number of hydroxyl groups. Fig. 8, *E* and *F* illustrate the contrasting capacity of PG and GLY, respectively, to maintain the structural integrity of a bilayer at 15.0 mol. %.

Investigation of the average coordination of nitrogen atoms of the lipid headgroups by water molecules can provide information about the solvation of the bilayer at the lipid/water interface [66]. Fig. 9 shows the water coordination of the nitrogen atoms of lipid phosphate groups for the different cryosolvents as a function of concentration. A steady decline in the coordination number is observed for all systems as the cryosolvent concentration is increased, indicating that the lipid headgroups are being dehydrated. For the alcohol species, this level of dehydration is shown to depend upon the number of hydroxyl groups present in each cryosolvent molecule, whereby the greater the number of hydroxyl groups the greater the displacement of water molecules. Interestingly, despite the inability of DMSO to form hydrogen bonds to lipids, the build-up of DMSO at the bilayer interface causes water molecules to be displaced, leading to a reduction in the number of water molecules that are hydrogen bonded to the DPPC molecules.

The average coordination of the carbonyl oxygen atoms of the lipid ester groups by water molecules provides insight into the solvation of the glycerol region of the bilayer. The results in Table 3 show the water coordination of one of the carbonyl oxygen atoms in the presence of cryosolvents as a function of concentration, and highlights the ability of each alcohol to readily displace water molecules at these regions, with GLY having the most pronounced

effect on water displacement across all concentrations, followed by PG, EG and MET in that order respectively (a similar result is observed for the second ester group of the lipid; not shown). Comparatively, DMSO cannot hydrogen bond with these regions hence the reduced capacity of DMSO to replace water molecules at these sites relative to the alcohols.

Fig. 10 illustrates the deuterium order parameter, SCD, of the *sn*-2 phospholipid chains for bilayer systems in the presence of cryosolvents at different concentrations. The ordering of the phospholipid chains decreases as the concentration of MET increases - a trend described as indirectly proportional to the increasing APL, affording more flexibility to the lipid acyl tails and leading to membrane thinning [29]. A similar trend is noticed for the ordering of acyl chains of the lipids with added EG and PG, with the ordering of the chains decreasing as the alcohol concentration increases up to 10.0 mol. % . The ordering of the 15.0 mol. % systems shows little change from the 10.0 mol. % systems. Similar behaviour is also seen for the GLY systems, with the ordering of the acyl chains decreasing steadily up to a concentration of 10.0 mol. %, but above this point the ordering of the acyl chains is not depressed any further and, in fact, an increase in ordering of carbons 2-4 is observed. This behaviour of GLY is clarified in the subsequent paragraphs of this discussion *via* detailed analysis of the hydrogen bonding tendencies for the cryosolvent.

In the presence of each cryosolvent, the average number of hydrogen bonds between water molecules and the constituent phospholipid headgroups is inferred to decrease as the concentration of alcohol increases (Table 4). These observations are consistent with the computed coordination numbers (Table 3), suggesting that membrane dehydration occurs as a consequence of the interactions with the cryosolvent. At 10.0 mol. % DMSO is shown again, in Table 4, to have relatively lower capacity to dislodge water from lipid hydrogen-bond acceptor atoms in comparison to the results for hydroxylated cryosolvents. Compared to the investigated alcohols, the inability of DMSO to hydrogen bond to the lipid bilayer at these

sites of induced water displacement could indicate that the alcohols are less damaging to the DPPC bilayer than DMSO.

Analysis of the data in Table 4 shows that as the concentration of each hydroxylated cryosolvent increases, hydrogen bonding between these cryosolvents and constituent lipid groups increases, as expected. Converse to other polyhydroxylated cryosolvents, PG is shown to form more hydrogen bonds with the glycerol regions relative to the phosphate regions at 2.5 mol. %; however, this behaviour reverses as concentration increases to 15.0 mol. %. In agreement with the density profiles for PG and MET, the average hydrogen bonding of these cryosolvents at 2.5 mol. % suggests that they diffuse past the phosphate headgroups with greater ease than EG and GLY to display an aggregating tendency at the glycerol regions of the bilayer. For PG and MET, hydrogen bonding is not specifically the underlying interaction driving them towards these more-submerged glycerol regions of a bilayer, but rather it is the substitution of water molecules from these regions to result in a favourable change in free energy [34]. Low concentrations of MET and PG (2.5 mol. %) thus result in a slight preferential tendency of these molecules to aggregate and hydrogen bond at the ester regions of lipid glycerol headgroups as a reflection of this favourable free energy change. A similar behaviour for MET at low concentrations has been reported earlier [29, 40], suggesting that, as a consequence of this behaviour, the action of MET is to provide stability to the dehydrated bilayer *via* intercalation at the interior ester region of the phospholipids.

The only other MD simulation study of MET interacting with a DPPC bilayer at high concentrations (23.5 mol. %, [34]) suggested that the tendency of this alcohol to aggregate at the ester regions of the bilayer is maintained, leading to lateral pressure on the membrane bilayer due to an increased number of MET molecules vying for the non-polar regions of the membrane interior, inducing frequent transmembrane crossing events as a consequence of the compromised structure of the membrane [34]. However, in this study of MET a shared hydrogen bonding preference to both lipid acceptor sites is largely maintained at high

concentrations, whilst an aggregating tendency of the alcohol towards the phosphate headgroups appears to prevail at concentrations beyond 10.0 mol. %, resulting in a relatively less pronounced decrease in structural ordering of the bilayer and thus fewer transmembrane crossing events (three cryosolvent molecules were observed to cross the membrane at 25.0 mol. % during a 60 ns period). Similar to MET, an aggregating affinity shift from the glycerol to the phosphate groups is observed for PG at concentrations of 5.0 mol. % and above (up to 15.0 mol. %). Such a change can be seen from the relative increase in cryosolvent-phosphate hydrogen bonding. It is proposed that the observed binding affinity shift is the result of an increase in disorder of the membrane structure (evidenced by Fig. 10), leading to enhanced accessibility of the phosphate groups to the cryosolvents, relative to the glycerol groups.

Despite a change in the preferential aggregation tendency of MET, continuous membrane lateral expansion and thinning resulting in a steady decrease in membrane structural ordering at concentrations up to 25.0 mol. % suggests the existence of one largely consistent concentration-dependent regime for this cryosolvent. Preferential aggregation of MET stemming from the glycerol regions of a bilayer outwards to the phosphate headgroup regions leads to solvent replacement by MET at both sites of the bilayer (as shown in Table 3) resulting in membrane expansion laterally and membrane thinning longitudinally to reduce structural order of the membrane bilayer. As concentration is increased from 2.5 mol. % up to 25.0 mol. %, available hydrogen bonding sites at the ester regions of phospholipids become largely occupied by MET molecules such that the resulting solvent replacement at the bilayer surface induces further lateral expansion and thinning of the membrane and thus continues to decrease the structural order of the bilayer. At 25.0 mol. %, localised sections of the bilayer become compromised enough to allow rare transmembrane crossing events; however, the overall structure of the membrane remains intact.

Many of the reported effects in this study of MET interaction with the lipid bilayers (including significant lateral expansion of the membrane, continuous decrease in the order of acyl chains, penetration of MET beyond the lipid/water interface, and extensive substitution of water at hydrogen bonding sites of the bilayer) are typical of "alcohol-like" behaviour [34]. However, the change in the bilayer surface at increased concentrations of MET (>10.0 mol.%) characterised by more extensive substitutions of water molecules at the phosphate groups of the bilayer challenge the predefined notions attributed to alcohol-like behaviour, and provide a more detailed understanding of the action of MET in the analysed concentration range.

The average number of hydrogen bonds shown in Table 4 provides evidence consistent with analyses of density profiles to suggest an inability of EG and GLY across all concentrations to penetrate as deeply as MET and PG between phospholipids, resulting in greater hydrogen bonding and thus water substitution at the phosphate headgroups of the bilayer interface than at the glycerol headgroups. This tendency is consistent with studies conducted for these species at lower concentration regimes [7] and is indicative of the greater hydrophilic character of EG and GLY, allowing for a competitive advantage to displace higher polarity species such as water at the lipid/water interface of the bilayer [52].

Visual inspection of the 15.0 mol. % EG, PG and GLY systems, reveals dual bonding of individual cryosolvent molecules to one phospholipid headgroup, either at two glycerol moieties or between the phosphate and one glycerol moiety (Fig. 11, *A* and *B*), leading to ordering effects of the acyl chains. The effect of the observed hydrogen bonding capacity of these cryosolvents partially explains how structural disordering of the phospholipid acyl chains is less significant at increased concentrations.

Lipid cross-linking *via* the cryosolvent molecules PG and EG was infrequently observed at concentrations of 15.0 mol. %, either *via* two phosphate groups of different phospholipid or *via* two glycerol groups (Fig. 11, *C* and *D* respectively) with a relatively marginal effect on

lipid ordering. Upon cross-linking of these molecules between glycerol moieties of different phospholipids (Fig. 11, *D*), the cross-linked molecule was observed to be "shielded" from approaching solvent molecules *via* hydrophobic interactions between the choline group of each linked phospholipid and the hydrophobic regions of the cryosolvents. GLY molecules were observed to interact with multiple phospholipids at the ester sites of the acyl chains to induce lipid cross-linking in a similar fashion to PG and EG, but predominantly between the terminal hydroxyl groups of the cryosolvent (Fig. 11, *E* and *F*).

The specific bridging of lipids at ester sites *via* GLY molecules is proposed to induce a greater effect on lipid acyl chain ordering than EG and PG as a consequence of the increased distance between linked phospholipids resulting from the comparatively larger size of GLY molecules, and the fact that GLY molecules exhibit an extra hydrogen-bonding donor group that is capable of favourably orientating towards approaching cryosolvent molecules. In comparison to PG and EG, the GLY-induced bridging effect does not require "shielding" of a non-polar cryosolvent group from the attached choline headgroups, likely resulting in less molecular strain on the interacting phospholipids to allow for greater ordering of the lipid acyl chains.

The average number of hydrogen bonds per molecule of the cryosolvents to the phosphate and glycerol groups in the DPPC bilayer (Table 5) is consistent with the visual analysis of specific binding events, revealing that EG, PG and GLY form more than one hydrogen bond per molecule with the glycerol and phosphate regions of the bilayer, across all tested concentrations. MET can only form one hydrogen bond per molecule to each region of the bilayer and thus these results have been omitted from Table 5. Across all concentrations, each cryosolvent is shown to form more hydrogen bonds per molecule with the glycerol regions of the lipid bilayer than the phosphate regions. It is observed that as concentration increases beyond 2.5 mol. % for each cryosolvent species, bridging between lipid phosphate headgroups decreases dramatically – a possible outcome of the increased number of

competing cryosolvent molecules inhibiting dual-binding events. The dependence of cryosolvent hydroxide groups per molecule available to hydrogen bond is highlighted in Table 4, whereby GLY is observed to be more capable of inducing more hydrogen bonds per molecule than EG and PG, which are shown to share relatively analogous hydrogen bonding results for both regions of the lipid bilayer. As concentration of GLY increases to 15.0 mol. %, a decline in the number of hydrogen bonds to the glycerol headgroup per GLY molecule is observed, suggesting a decrease in the capacity for GLY molecules at these concentrations to induce multiple binding – again, a possible outcome of competing cryosolvent molecules inhibiting multiple-binding events at this region.

The results of Table 5 are consistent with the analysis of hydrogen bonding between the polyhydroxylated cryosolvents and lipid headgroups (Table 6), which reveals that specific dual-, and for GLY, triple-hydrogen bonding of individual cryosolvent molecules to multiple sites on one phospholipid or multiple phospholipids, occurs more frequently as concentration of cryosolvent increases, but decreases relative to the number of single-binding events. It is shown that GLY molecules induce more dual-hydrogen bonding events than PG and EG across all concentrations, with approximately half of all interacting GLY molecules being involved in multiple-hydrogen bonding at each concentration. A steady increase in multiple bonding between individual cryosolvent molecules and phospholipids occurs between 2.5 and 10.0 mol. % for all cryosolvents, before a relatively small increase in multiple-hydrogen bonding of phospholipids (or none at all) is observed at 15.0 mol. %. This finding for 15.0 mol. % may be indicative of a saturation point for multiple hydrogen bonding between individual cryosolvent molecules, wherein further multiple hydrogen bonding events are hindered by other cryosolvent molecules.

Analysis of the hydrogen bonding affinity (HBA) of the hydroxylated cryosolvents normalised for the number of hydrogen bond donor/acceptor groups per cryosolvent molecule (see Figs. 12, *A, B* and *C*) indicates that as the concentration of cryosolvent increases, all

species exhibit (1) a slight decreasing affinity for water molecules, (2) a decreasing affinity for the lipid bilayer up to concentrations of approximately 10.0 mol. %, and (3) an increasing affinity to other cryosolvent molecules. Of the alcohols, MET is noted to have the strongest affinity with water and the lowest affinity to other MET molecules and the bilayer up to 10.0 mol. %, which is consistent with the aggregating tendencies of MET in Fig. 7 and Fig. 8, *A*. The affinity of PG to other PG molecules is largely analogous to EG, whilst the affinity of PG to the DPPC bilayer is shown to be higher than the other cryosolvents, reflecting its greater lipophilicity. The stronger binding affinity of GLY to other GLY molecules in comparison to the cryosolvent-cryosolvent interactions for EG, PG and MET (Fig. 12 *B*) indicates that, as concentration increases, comparatively more GLY molecules are interacting with each other to reduce water interactions – including those GLY molecules hydrogen bonding to the bilayer by one or two hydroxyl groups.

The apparent decreasing affinity of all cryosolvents for the lipid bilayer (Fig. 12 B) is due to the fact that, as the concentration of cryosolvent increases, a larger proportion of these molecules self-aggregate (Fig. 12 C) and the coverage of the lipid bilayer gradually saturates. By contrast, analysis of the HBA of those cryosolvent molecules in the vicinity of the bilayer only (Fig. 12 D) reveals that GLY has an intrinsic (independent of concentration) higher affinity to the lipid bilayer than EG, PG and MET, in that order respectively, consistent with the increased capacity of GLY to hydrogen bond with multiple lipid headgroups (Table 6). This suggests the formation of a multi-layered cryosolvent deposit across the lipid membrane surface between GLY molecules interacting with the bilayer and a separate bulk phase containing GLY molecules interacting with other GLY molecules *via* available hydroxyl groups at high concentrations (as evidenced by the aggregation tendencies shown in Figs. 5 *E* and *F,* and the hydrogen bonding trends shown in Tables 5 and 6).

The contrasting trends for the binding affinities of PG, EG and MET to water molecules and other cryosolvent molecules (Fig 12 *A* and *B,* respectively) also suggests that,

analogously to GLY, these cryosolvents exhibit self-aggregation as the concentration increases, leading to a small reduction in water interactions. In the case of PG and EG, these HBA trends could suggest the formation of a multi-layered cryosolvent coating across the surface of the bilayer at sufficiently high concentrations (evidenced by the aggregating tendency of PG in Figs. 9, *C* and *D,* and the hydrogen bonding trends in Tables 5 and 6). In comparison to GLY, the lower capacity of PG and EG to hydrogen bond to other cryosolvent molecules (Tables 5 and 6), along with the slightly stronger affinity to water of EG (Fig 12. *A*), is likely to lessen this effect. The lack of an extra hydrogen bond donor group renders MET incapable of forming a multi-layered cryosolvent coating in the same fashion as the polyhydroxylated cryosolvents, as reflected in the comparatively higher affinity of MET to water molecules in Fig. 12, *A,* and the subsequent lower affinity to other MET molecules in Fig. 12, *B*.

At concentrations similar to 10.0 mol. %, EG and GLY (13.3 and 10.3 mol. %, respectively) have been described in earlier reports to display intrinsically distinct behaviour in a lipid bilayer environment: EG behaved in an “alcohol-like” fashion by interacting preferentially with the ester regions of the bilayer, whilst GLY was described as having neither alcohol- nor sugar-like behaviour and was largely inert with respect to the membrane [34]. By contrast, EG and GLY were shown in this current study to maintain a preferential aggregating and hydrogen bonding tendency to the phosphate headgroups of the bilayer (relative to the number of hydroxyl groups in each molecule), to induce further APL increases, membrane lateral expansion and thinning, and solvent displacement at the lipid/water interface.

It is clear from the order parameter analyses that EG, PG and GLY exhibit behavioural changes at concentrations exceeding 10.0 mol. %, and two regimes for each species are identified based on the concentration regimes investigated. For EG and GLY at low to moderate concentrations (2.5 – 10.0 mol. %), preferential affinity to the bilayer surface leads

to extensive substitution of water molecules at the lipid/water interface of the lipid bilayer, resulting in increased hydrogen bonding between the cryosolvent hydroxyl groups and (predominantly) the phosphate groups of the phospholipids, ultimately inducing significant lateral expansion of the membrane and decreased order parameters of the lipid acyl chains consistently with increasing cryosolvent concentration. A similar trend is noticed for PG at concentrations between 5.0 and 10.0 mol. %, once available ester sites are occupied by PG in a similar fashion to the saturating effects of MET at sufficient concentrations.

At concentrations of 15.0 mol. % the three polyhydroxylated cryosolvents (EG, PG and GLY) continued to interact predominantly with the phospholipid headgroup region of the bilayer, leading to the formation of a coating layer of cryosolvent molecules along the surface of the membrane, as evidenced by MDPs and the average number of hydrogen bonds. However, the increased APL resulting from a larger number of cryosolvent molecules competing at the lipid/water interface to reduce polar interactions with water leads to an increase in cryosolvent bilayer penetration and thus specific interactions with the ester regions of the phospholipid headgroups are induced. Increased concentrations of PG and EG induce consistent - and for the specific case of PG, relatively more pronounced - increases in APL, although there is little evidence to suggest the development of a membrane lipid phase transition or structural disordering, as found for DMSO experimentally at relative concentrations under such conditions [49]. The ability of EG and PG at high concentrations to interact with the lipid bilayer without destroying the integrity of its liquid crystalline characteristics suggests that the specific binding affinity and aggregating tendency of these cryosolvents acts to provide enhanced structural support to the phospholipid bilayer.

The capacity of these three polyhydroxylated cryosolvents to bind to multiple phospholipid sites was shown to induce specific changes in phospholipid acyl chain ordering, cross-linking of multiple phospholipids (predominantly *via* the ester regions of the lipids), and the formation of a surface coating, at sufficiently high concentrations. It is proposed that the

relatively superior capacity of GLY molecules to induce multiple, specific binding events leading to cross-linking of phospholipids between phospholipid glycerol moieties up to 15.0 mol. %, coupled with increased affinity to other cryosolvent molecules leading to the formation of a dense bilayer-surface coating, reduces the structural disordering effect on the bilayer stemming from membrane lateral expansion and thinning.

4. Conclusions

The systematic molecular dynamics simulations study of the effects of MET, PG, EG, GLY and DMSO on a hydrated liquid crystalline DPPC bilayer provided an atomic-scale representation of the diffusional and aggregating tendencies of these cryosolvent species and their consequent effects on the bilayer. The trends observed for each alcohol and DMSO were found to describe regimes dependent on the size, hydrophobicity and concentration of cryosolvent, expanding the established notions of alcohol-like and sugar-like behaviours for these cryosolvent species [34]. The lower dipole moment compared with water of each cryosolvent species encouraged interaction at the membrane interface leading to the displacement of water from the phosphate and glycerol headgroups of the phospholipids resulting in hydrogen bonding at these sites.

Each cryosolvent induced concurrent membrane lateral expansion and thinning normal to the bilayer, with this effect increasing for all cryosolvents as the concentration increased. Of the alcohols investigated, the effect of membrane lateral expansion was shown to be greatest for PG, which behaved in an analogous fashion to DMSO at equivalent concentrations under the same conditions up to 10.0 mol. %. Beyond 10.0 mol. %, DMSO has been shown experimentally to induce lipid phase changes under similar conditions [49],whilst in this study PG was observed to continue to expand the membrane laterally up to 15.0 mol. % without penetrating as deeply into the membrane interior, nor in the same quantity, as DMSO at 10.0 mol. %. MET, EG and GLY were shown to induce less pronounced membrane lateral

expansion and thinning normal to the bilayer in a relatively comparable fashion up to concentrations of 15.0 mol. %, and were generally not observed to penetrate beyond the lipid headgroups.

Structural ordering of the membrane bilayer was shown to decrease relative to concentration for all alcohols. Again, this effect was most pronounced for PG, whilst MET, EG and GLY were noted to induce relatively similar membrane structural disordering across the tested concentrations. As a consequence, this effect was shown to be relative to the hydrophobicity of the cryosolvent species under the investigated conditions, with PG being more lipophilic than MET, EG and GLY. As a consequence of their relative hydrophobicity, PG and MET display a stronger tendency than EG and GLY to aggregate towards the glycerol regions of the phospholipid headgroups across all concentrations. This tendency leads to an increased ability to substitute water molecules at these ester sites first before water substitution can occur at the phosphate regions of phospholipid headgroups. The reverse trend was noticed for EG and GLY across all tested concentrations.

As concentrations of MET increased to 25.0 mol. %, a consistent decrease in phospholipid acyl chain ordering was recorded. The same trend was observed for the remaining cryosolvents up to concentrations of 10.0 mol. %. At concentrations beyond 10.0 mol. %, PG and EG were shown to induce a much less significant decrease in acyl chain ordering as a consequence of specific interactions resulting from individual cryosolvent molecules hydrogen bonding predominantly to two glycerol groups of the one phospholipid. Cross-linking between GLY molecules and these ester regions of phospholipids was observed between the terminal hydroxyl groups of the cryosolvent, leaving the secondary hydroxyl group of GLY free to interact with the solvent environment. The capacity of GLY to cross-link lipid molecules in this fashion was observed to impose ordering of the phospholipid acyl chain, whilst increased GLY-GLY interactions at the interface of the lipid membrane led to the formation of a dense cryosolvent coating layer along the surface of the bilayer. As a

consequence, a relative conservation of the membrane structural order was achieved across tested concentrations.

The ability to determine the effects of MET, EG, PG, GLY and DMSO on a DPPC phospholipid bilayer at a molecular level *via* MD simulations has provided insight into the specific mechanism of action of each cryosolvent in ways that have proved difficult or impossible to determine using experimental techniques. Investigation of the concentration dependence of each species to induce membrane structural change has provided a gateway towards informing future cryopreservation protocols involving these cryosolvents. In particular, this research has described the mode of action of PG to be analogous to DMSO without penetrating as deeply as DMSO towards the bilayer interior at equivalent concentrations, nor compromising the structural integrity of the membrane at concentrations up to 15.0 mol. %. In addition, the formation of a protective cryosolvent layer along the surface of the membrane suggests that PG could be used in cryoprotection protocols as a potentially less damaging substitute for DMSO.

Acknowledgements

This research was supported by the Australian Research Council (ARC) Linkage Grant LP00884027 with further financial support from Alcoa of Australia Ltd and BHP Billiton Worsley Alumina Pty Ltd. The computational resources utilised for this research project were provided by iVEC.

References

[1] A. Kaczmarczyk, B. Funnekotter, A. Menon, P.Y. Phang, A. Al-Hanbali, E. Bunn, R.L. Mancera, Current issues in plant cryopreservation, in: I.I. Katkov (Ed.) Current Frontiers in Cryobiology, InTech Open Access Publisher, 2012, pp. 417-438.
[2] A. Kaczmarczyk, S. Turner, E. Bunn, R.L. Mancera, K. Dixon, Cryopreservation of threatened native Australian species—what have we learned and where to from here?, In Vitro Cellular & Developmental Biology - Plant, 47 (2011) 17-25.
[3] J. Wolfe, G. Bryant, Cellular cryobiology: thermodynamic and mechanical effects, International Journal of Refrigeration, 24 (2001) 438-450.
[4] J.B. Mandumpal, C.A. Kreck, R.L. Mancera, A molecular mechanism of solvent cryoprotection in aqueous DMSO solutions, Phys Chem Chem Phys, 13 (2011) 3839-3842.
[5] C.A. Kreck, J.B. Mandumpal, R.L. Mancera, Prediction of the glass transition in aqueous solutions of simple amides by molecular dynamics simulations, Chemical Physics Letters, 501 (2011) 273-277.
[6] L.E. McGann, Differing actions of penetrating and nonpenetrating cryoprotective agents, Cryobiology, 15 (1978) 382-390.
[7] A. Kyrychenko, T.S. Dyubko, Molecular dynamics simulations of microstructure and mixing dynamics of cryoprotective solvents in water and in the presence of a lipid membrane, Biophys Chem, 136 (2008) 23-31.
[8] C. Robinson, C.S. Boxe, M.I. Guzmán, A.J. Colussi, M.R. Hoffmann, Acidity of Frozen Electrolyte Solutions, The Journal of Physical Chemistry B, 110 (2006) 7613-7616.
[9] G. Bryant, K.L. Koster, J. Wolfe, Membrane behaviour in seeds and other systems at low water content: the various effects of solutes, Seed Science Research, 11 (2007) 17-25.
[10] J. Wolfe, G. Bryant, Freezing, Drying, and/or Vitrification of Membrane– Solute–Water Systems, Cryobiology, 39 (1999) 103-129.
[11] K.L. Koster, Glass formation and desiccation tolerance in seeds, Plant Physiology, 96 (1991) 302.
[12] J. Wolfe, Lateral Stresses in Membranes at Low Water Potential, Functional Plant Biology, 14 (1987) 311-318.
[13] I. Puhlev, N. Guo, D.R. Brown, F. Levine, Desiccation tolerance in human cells, Cryobiology, 42 (2001) 207-217.
[14] B. Kent, C.J. Garvey, T. Lenné, L. Porcar, V.M. Garamus, G. Bryant, Measurement of glucose exclusion from the fully hydrated DOPE inverse hexagonal phase, Soft Matter, 6 (2010) 1197.
[15] G. Bryant, J. Wolfe, Interfacial Forces in Cryobiology and Anhydrobiology, Cryoletters, 13 (1992) 23-36.
[16] K.L. Koster, A.C. Leopold, Sugars and desiccation tolerance in seeds, Plant Physiology, 88 (1988) 829-832.
[17] R.L. Mancera, M. Chalaris, K. Refson, J. Samios, Molecular dynamics simulation of dilute aqueous DMSO solutions. A temperature-dependence study of the hydrophobic and hydrophilic behaviour around DMSO, Physical Chemistry Chemical Physics, 6 (2004) 94-102.
[18] R.L. Mancera, M. Chalaris, J. Samios, The concentration effect on the 'hydrophobic' and 'hydrophilic' behaviour around DMSO in dilute aqueous DMSO solutions. A computer simulation study, Journal of Molecular Liquids, 110 (2004) 147-153.
[19] R.L. Mancera, M. Chalaris, J. Samios, Recent advances in the understanding of hydrophobic and hydrophilic effects: A theoretical and computer simulation perspective., in: J. Samios, V.A. Durov (Eds.) Novel Approaches to the Structure and Dynamics of Liquids: Experiments, Theories and Simulations., NATO Science Series, 2004, pp. 387-396.
[20] T.J. Anchordoguy, J.F. Carpenter, J.H. Crowe, L.M. Crowe, Temperature-dependent perturbation of phospholipid bilayers by dimethylsulfoxide, Biochimica et Biophysica Acta (BBA) - Biomembranes, 1104 (1992) 117-122.
[21] A. Menon, B. Funnekotter, A. Kaczmarczyk, E. Bunn, S. Turner, R.L. Mancera, Cryopreservation of Lomandra sonderi (asparagaceae) shoot tips using droplet-vitrification, Cryoletters, 34 (2012) 259-270.
[22] Z.E. Hughes, A.E. Mark, R.L. Mancera, Molecular dynamics simulations of the interactions of DMSO with DPPC and DOPC phospholipid membranes, The Journal of Physical Chemistry B, 116 (2012) 11911-11923.
[23] A.A. Gurtovenko, J. Anwar, Modulating the structure and properties of cell membranes: the molecular mechanism of action of dimethyl sulfoxide, The Journal of Physical Chemistry B, 111 (2007) 10453-10460.
[24] A.A. Gurtovenko, J. Anwar, Ion transport through chemically induced pores in protein-free phospholipid membranes, The Journal of Physical Chemistry B, 111 (2007) 13379-13382.
[25] A.A. Gurtovenko, J. Anwar, I. Vattulainen, Defect-mediated trafficking across cell membranes: insights from in silico modeling, Chemical Reviews, 110 (2010) 6077-6103.
[26] A.A. Gurtovenko, O.I. Onike, J. Anwar, Chemically induced phospholipid translocation across biological membranes, Langmuir, 24 (2008) 9656-9660.

[27] R. Notman, M. Noro, B. O'Malley, J. Anwar, Molecular basis for dimethylsulfoxide (DMSO) action on lipid membranes, Journal of the American Chemical Society, 128 (2006) 13982-13983.
[28] A.K. Sum, J.J. de Pablo, Molecular simulation study on the influence of dimethylsulfoxide on the structure of phospholipid bilayers, Biophys J, 85 (2003) 3636-3645.
[29] B.W. Lee, R. Faller, A.K. Sum, I. Vattulainen, M. Patra, M. Karttunen, Structural effects of small molecules on phospholipid bilayers investigated by molecular simulations, Fluid phase equilibria, 225 (2004) 63-68.
[30] Z.E. Hughes, R.L. Mancera, Molecular dynamics simulations of mixed DOPC–β-sitosterol bilayers and their interactions with DMSO, Soft Matter, 9 (2013) 2920-2935.
[31] Q. Dong, J. Lin, C. Huang, Effects of cryoprotectant toxicity on the embryos and larvae of pacific white shrimp Litopenaeus vannamei, Aquaculture, 242 (2004) 655-670.
[32] T. Mukaida, S. Wada, K. Takahashi, P. Pedro, T. An, M. Kasai, Vitrification of human embryos based on the assessment of suitable conditions for 8-cell mouse embryos, Human reproduction, 13 (1998) 2874-2879.
[33] C.A. Kreck, R.L. Mancera, Molecular dynamics simulations of the glass transition in aqueous polyol solutions, Manuscript in progress., (2013).
[34] C.S. Pereira, P.H. Hünenberger, The influence of polyhydroxylated compounds on a hydrated phospholipid bilayer: a molecular dynamics study, Molecular Simulation, 34 (2008) 403-420.
[35] B.J. Fuller, Cryoprotectants: the essential antifreezes to protect life in the frozen state, Cryoletters, 25 (2004) 375-388.
[36] Z. Hubálek, Protectants used in the cryopreservation of microorganisms, Cryobiology, 46 (2003) 205-229.
[37] B.W. Barry, Mode of action of penetration enhancers in human skin, Journal of Controlled Release, 6 (1987) 85-97.
[38] L. Löbbecke, G. Cevc, Effects of short-chain alcohols on the phase behavior and interdigitation of phosphatidylcholine bilayer membranes, Biochimica et Biophysica Acta (BBA) - Biomembranes, 1237 (1995) 59-69.
[39] M. Hagedorn, Magnetic resonance microscopy and spectroscopy reveal kinetics of cryoprotectant permeation in a multicompartmental biological system, Proceedings of the National Academy of Sciences of the United States of America, 93 (1996) 7454.
[40] M. Patra, E. Salonen, E. Terama, I. Vattulainen, R. Faller, B.W. Lee, J. Holopainen, M. Karttunen, Under the influence of alcohol: the effect of ethanol and methanol on lipid bilayers, Biophys J, 90 (2006) 1121-1135.
[41] D. Bemporad, J.W. Essex, C. Luttmann, Permeation of small molecules through a lipid bilayer: a computer simulation study, The Journal of Physical Chemistry B, 108 (2004) 4875-4884.
[42] H.V. Ly, M.L. Longo, The influence of short-chain alcohols on interfacial tension, mechanical properties, area/molecule, and permeability of fluid lipid bilayers, Biophys J, 87 (2004) 1013-1033.
[43] R.V. McDaniel, Nonelectrolyte substitution for water in phosphatidylcholine bilayers, Biochimica et biophysica acta. Biomembranes, 731 (1983) 97.
[44] M.J. Swamy, D. Marsh, Thermodynamics of interdigitated phases of phosphatidylcholine in glycerol, Biophys J, 69 (1995) 1402-1408.
[45] W.P. Williams, P.J. Quinn, L.I. Tsonev, R.D. Koynova, The effects of glycerol on the phase behaviour of hydrated distearoylphosphatidylethanolamine and its possible relation to the mode of action of cryoprotectants, Biochimica et biophysica acta. Biomembranes, 1062 (1991) 123-132.
[46] M. Yamazaki, M. Ohshika, N. Kashiwagi, T. Asano, Phase transitions of phospholipid vesicles under osmotic stress and in the presence of ethylene glycol, Biophys Chem, 43 (1992) 29-37.
[47] K. Nicolay, E.B. Smaal, B. de Kruijff, Ethylene glycol causes acyl chain disordering in liquid-crystalline, unsaturated phospholipid model membranes, as measured by 2H NMR, FEBS Letters, 209 (1986) 33-36.
[48] B. Bechinger, P.M. Macdonald, J. Seelig, Deuterium NMR studies of the interactions of polyhydroxyl compounds and of glycolipids with lipid model membranes, Biochimica et Biophysica Acta (BBA) - Biomembranes, 943 (1988) 381-385.
[49] S.N. Shashkov, M.A. Kiselev, S.N. Tioutiounnikov, A.M. Kiselev, P. Lesieur, The study of DMSO/water and DPPC/DMSO/water system by means of the X-ray, neutron small-angle scattering, calorimetry and IR spectroscopy, Physica. B: Condensed Matter, 271 (1999) 184-191.
[50] Z.E. Hughes, C.J. Malajczuk, R.L. Mancera, The Effects of Cryosolvents on DOPC-b-Sitosterol Bilayers Determined From Molecular Dynamics Simulations, The Journal of Physical Chemistry B, (2013) 3362-3375.
[51] D. Pinisetty, D. Moldovan, R. Devireddy, The effect of methanol on lipid bilayers: an atomistic investigation, Annals of Biomedical Engineering, 34 (2006) 1442-1451.
[52] D.P. Geerke, W.F. van Gunsteren, P.H. Hünenberger, Molecular dynamics simulations of the interaction between polyhydroxylated compounds and Lennard-Jones walls: preferential affinity/exclusion effects and their relevance for bioprotection, Molecular Simulation, 36 (2010) 708-728.
[53] D. Van Der Spoel, E. Lindahl, B. Hess, G. Groenhof, A.E. Mark, H.J. Berendsen, GROMACS: fast, flexible, and free, J Comput Chem, 26 (2005) 1701-1718.

[54] D. Poger, W.F. Van Gunsteren, A.E. Mark, A new force field for simulating phosphatidylcholine bilayers, J Comput Chem, 31 (2009) 1117-1125.
[55] D. Poger, A.E. Mark, On the validation of molecular dynamics simulations of saturated and cis-monounsaturated phosphatidylcholine lipid bilayers: a comparison with experiment, Journal of Chemical Theory and Computation, 6 (2009) 325-336.
[56] N. Schmid, A.P. Eichenberger, A. Choutko, S. Riniker, M. Winger, A.E. Mark, W.F. van Gunsteren, Definition and testing of the GROMOS force-field versions 54A7 and 54B7, Eur Biophys J, 40 (2011) 843-856.
[57] H.J. Berendsen, J.P.M. Postma, W.F. Van Gunsteren, J. Hermans, Interaction models for water in relation to protein hydration, Intermolecular Forces, 11 (1981) 331-338.
[58] C. Oostenbrink, A. Villa, A.E. Mark, W.F. van Gunsteren, A biomolecular force field based on the free enthalpy of hydration and solvation: the GROMOS force-field parameter sets 53A5 and 53A6, J Comput Chem, 25 (2004) 1656-1676.
[59] A.K. Malde, L. Zuo, M. Breeze, M. Stroet, D. Poger, P.C. Nair, C. Oostenbrink, A.E. Mark, An Automated Force Field Topology Builder (ATB) and Repository: Version 1.0, Journal of Chemical Theory and Computation, 7 (2011) 4026-4037.
[60] S.N. Shashkov, M.A. Kiselev, S.N. Tioutiounnikov, A.M. Kiselev, P. Lesieur, The study of DMSO/water and DPPC/DMSO/water system by means of the X-ray, neutron small-angle scattering, calorimetry and IR spectroscopy, Physica. B, Condensed matter, 271 (1999) 184-191.
[61] H.J.C. Berendsen, J.P.M. Postma, W.F. van Gunsteren, A. DiNola, J.R. Haak, Molecular dynamics with coupling to an external bath, The Journal of Chemical Physics, 81 (1984) 3684.
[62] M.P. Allen, D.J. Tildesley, Computer simulation of liquids, in, Clarendon Press 1989, pp. 80.
[63] W. Shinoda, S. Okazaki, A Voronoi analysis of lipid area fluctuation in a bilayer, The Journal of Chemical Physics, 109 (1998) 1517.
[64] M. Patra, M. Karttunen, M.T. Hyvönen, E. Falck, P. Lindqvist, I. Vattulainen, Molecular dynamics simulations of lipid bilayers: major artifacts due to truncating electrostatic interactions, Biophys J, 84 (2003) 3636.
[65] N. Kučerka, J.F. Nagle, J.N. Sachs, S.E. Feller, J. Pencer, A. Jackson, J. Katsaras, Lipid bilayer structure determined by the simultaneous analysis of neutron and X-ray scattering data, Biophys J, 95 (2008) 2356.
[66] L. Saiz, M.L. Klein, Structural properties of a highly polyunsaturated lipid bilayer from molecular dynamics simulations, Biophys J, 81 (2001) 204.

Fig. 1. Molecular structures of the hydroxoylated cryosolvents methanol (MET), propylene glycol (PG), ethylene glycol (EG) and glycerol (GLY).

Fig. 2. APL as a function of time for each cryosolvent at a concentration of 15.0 mol. % in a 128 DPPC bilayer system.

Fig. 3. APL as a function of cryosolvent concentration (up to 15.0 mol. %) in a 128 DPPC bilayer system.

Fig. 4. Comparison between the effects of alcohols and DMSO on DPPC membrane thickness (measured as the average distance between phosphate headgroups between the two leaflets) as a function of concentration of cryosolvent.

Fig. 5. MDPs perpendicular to the plane of the DPPC bilayers in solutions of (*A*) 0, (*B*) 2.5, (*C*) 10.0 and (*D*) 15.0 mol. % PG, and (*E*) 10.0 and (*F*) 15.0 mol. % GLY.

Fig. 6. MDPs perpendicular to the plane of the DPPC membranes without cryosolvent, and in the presence of (*A*) no cryosolvent, and (*B*) MET, (*C*) EG (*D*) GLY, (*E*) PG, and (*F*) DMSO, at 10.0 mol. %.

Fig. 7. The number density profiles for each concentration of cryosolvent in the DPPC bilayer system.

Fig. 8. Configuration snapshots taken from simulations of a DPPC bilayer in the presence of 2.5 mol. % *(A)* MET, *(B)* EG, *(C)* PG, *(D)* GLY, and 15.0 mol. % *(E)* PG, and *(F)* GLY. MET, EG, PG and GLY are coloured green, pink, orange and blue, respectively. All

phospholipid phosphate groups are coloured red, and the phospholipid tail groups are coloured cyan.

Fig. 9. Water coordination numbers for nitrogen atoms in the DPPC headgroups as a function of molar concentration of each cryosolvent.

Fig. 10. Deuterium order parameters for *sn*-2 chains for DPPC bilayer systems in the presence of *(A)* MET, *(B)* EG, *(C)* PG, and *(D)* GLY across a range of concentrations.

Fig. 11. Snapshots taken from the y-direction of *(A)* an EG molecule interacting with the two glycerol moieties of one DPPC phospholipid, *(B)* a PG molecule interacting with one glycerol moiety and one phosphate moiety of one DPPC phospholipid, *(C)* cross-linking of two DPPC phospholipids at their respective phosphate groups *via* a PG molecule, *(D)* cross-linking of two DPPC phospholipids at their glycerol groups *via* an EG molecule, and *(E)* cross-linking of phospholipids *via* a GLY molecule interacting with two DPPC phospholipids. A snapshot of the same cross-linking event involving GLY taken from the z-direction is shown in *(F)*. All oxygen groups are coloured in red, hydrogen groups in white, carbon groups in grey, phosphate groups in gold, and nitrogen groups in blue.

Fig. 12. Hydrogen bonding affinity (HBA) of the cryosolvents to *(A)* water, *(B)* cryosolvent molecules, *(C)* the DPPC lipid bilayer, normalised for cryosolvent hydrogen-bond donor groups, and (*D)* in the vicinity of the bilayer to the DPPC headgroups.

Table 1. DPPC membrane thickness (measured as the average distance between phosphate headgroups between the two leaflets) and APL as a measure of cryosolvent concentration.

Table 2. Bulk-to-peak height ratios of the cryosolvents MET, EG, PG and GLY in DPPC bilayer systems.

Table 3. Water coordination numbers for carbonyl oxygen of the DPPC glycerol headgroup as a function of mol percentage of each cryosolvent.

Table 4. Average total number of hydrogen bonds between the cryosolvents (MET, EG, GLY and DMSO) and water with the glycerol and phosphate headgroups of a DPPC bilayer, calculated for each 60 ns simulation of a DPPC bilayer in the absence or presence of different cryosolvents.

Table 5. The average number of hydrogen bonds that a cryosolvent molecule hydrogen bonded to the DPPC bilayer forms with the glycerol and phosphate groups, calculated and averaged from 10 snapshots across a 60 ns period.

Table 6. The number of double and triple hydrogen bonds formed between cryosolvent molecules and the DPPC molecules for ethylene glycol, propylene glycol and glycerol.

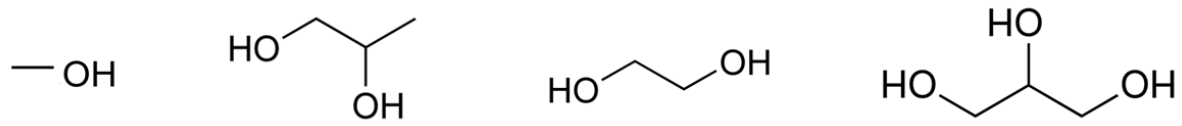

Fig. 1. Molecular structures of the hydroxoylated cryosolvents methanol (MET), propylene glycol (PG), ethylene glycol (EG) and glycerol (GLY).

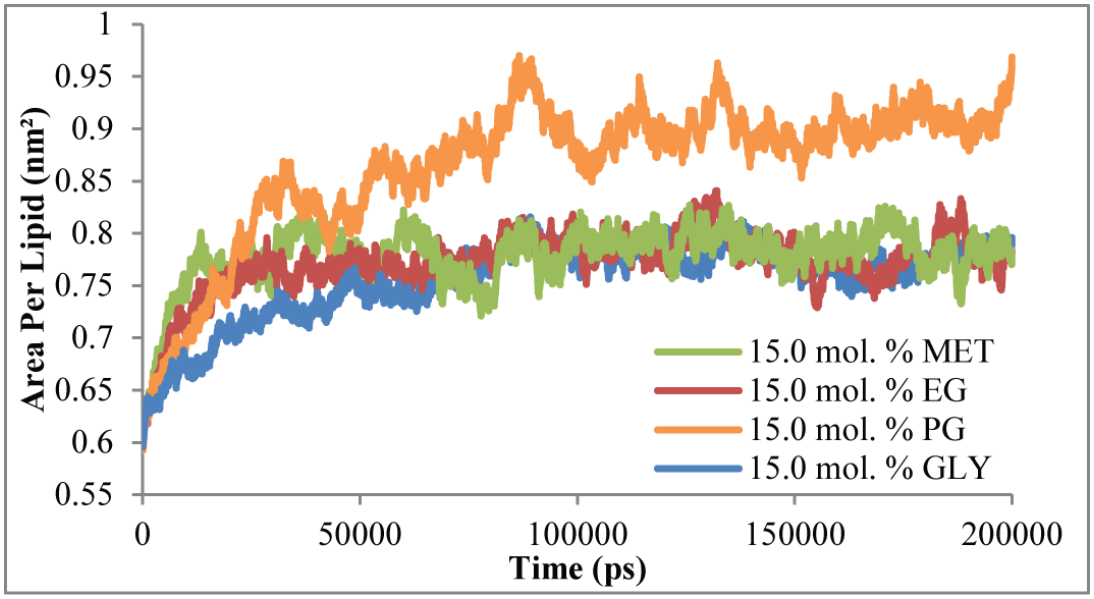

Fig. 2. APL as a function of time for each cryosolvent at a concentration of 15.0 mol. % in a 128 DPPC bilayer system.

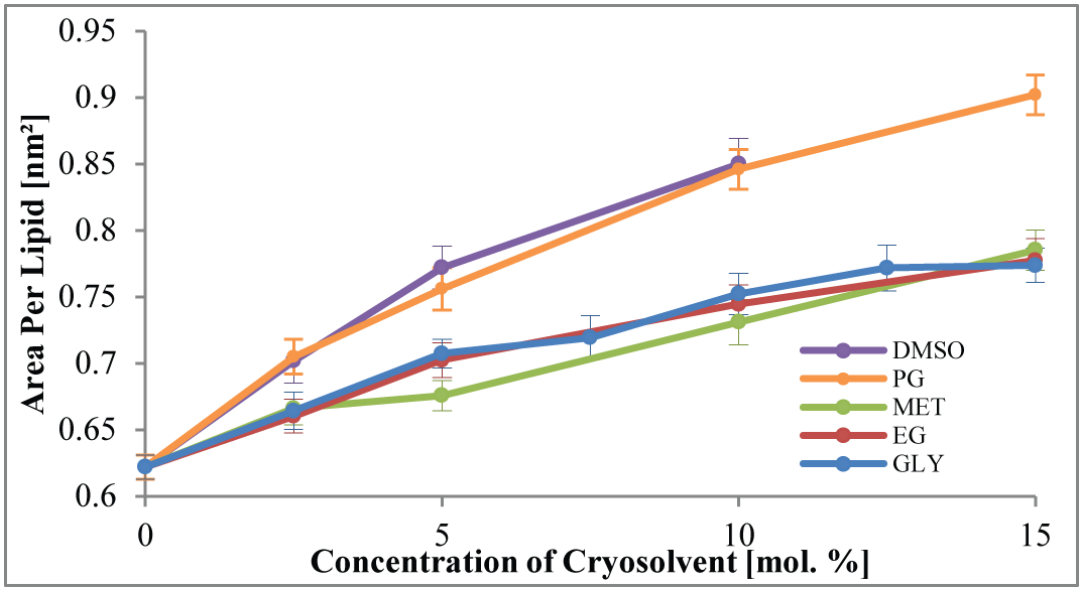

Fig. 3. APL as a function of cryosolvent concentration (up to 15.0 mol. %) in a 128 DPPC bilayer system.

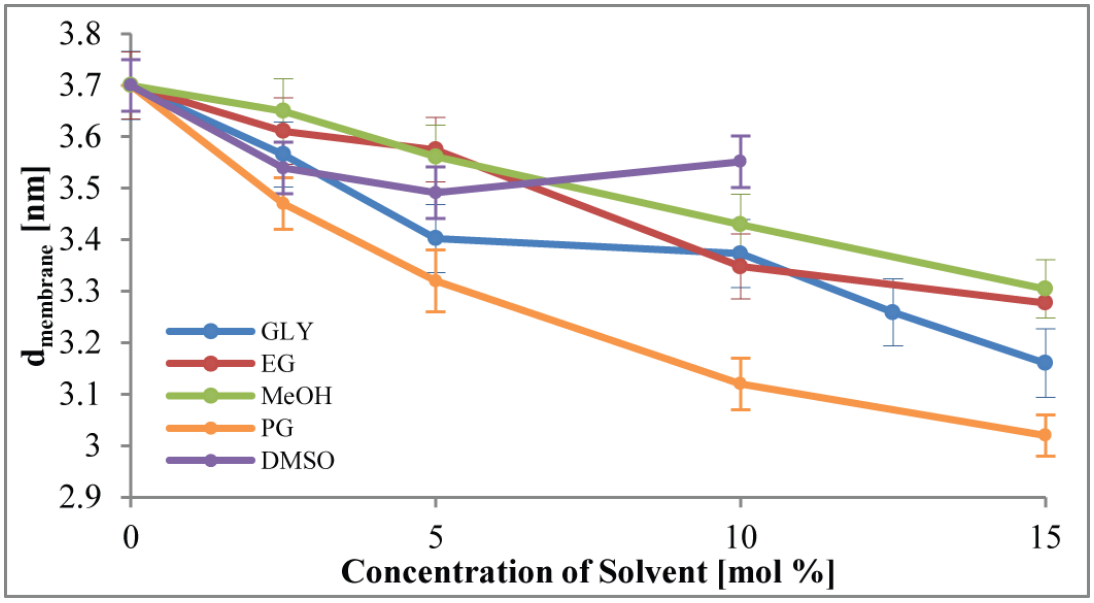

Fig. 4. Comparison between the effects of alcohols and DMSO on DPPC membrane thickness (measured as the average distance between phosphate head groups between the two leaflets) as a function of concentration of cryosolvent.

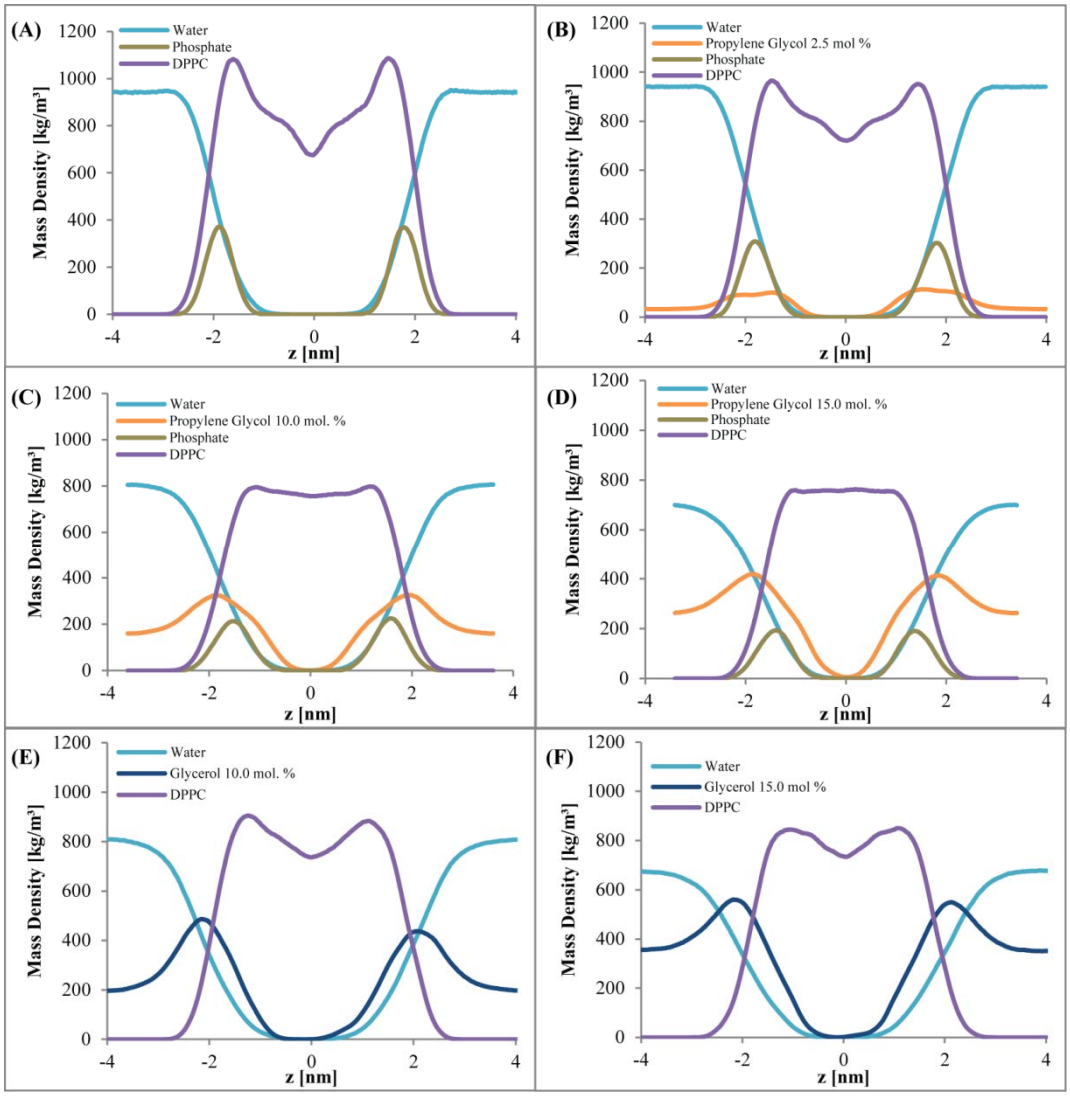

Fig. 5. MDPs perpendicular to the plane of the DPPC bilayers in solutions of (*A*) 0, (*B*) 2.5, (*C*) 10.0 and (*D*) 15.0 mol. % PG, and (*E*) 10.0 and (*F*) 15.0 mol. % GLY.

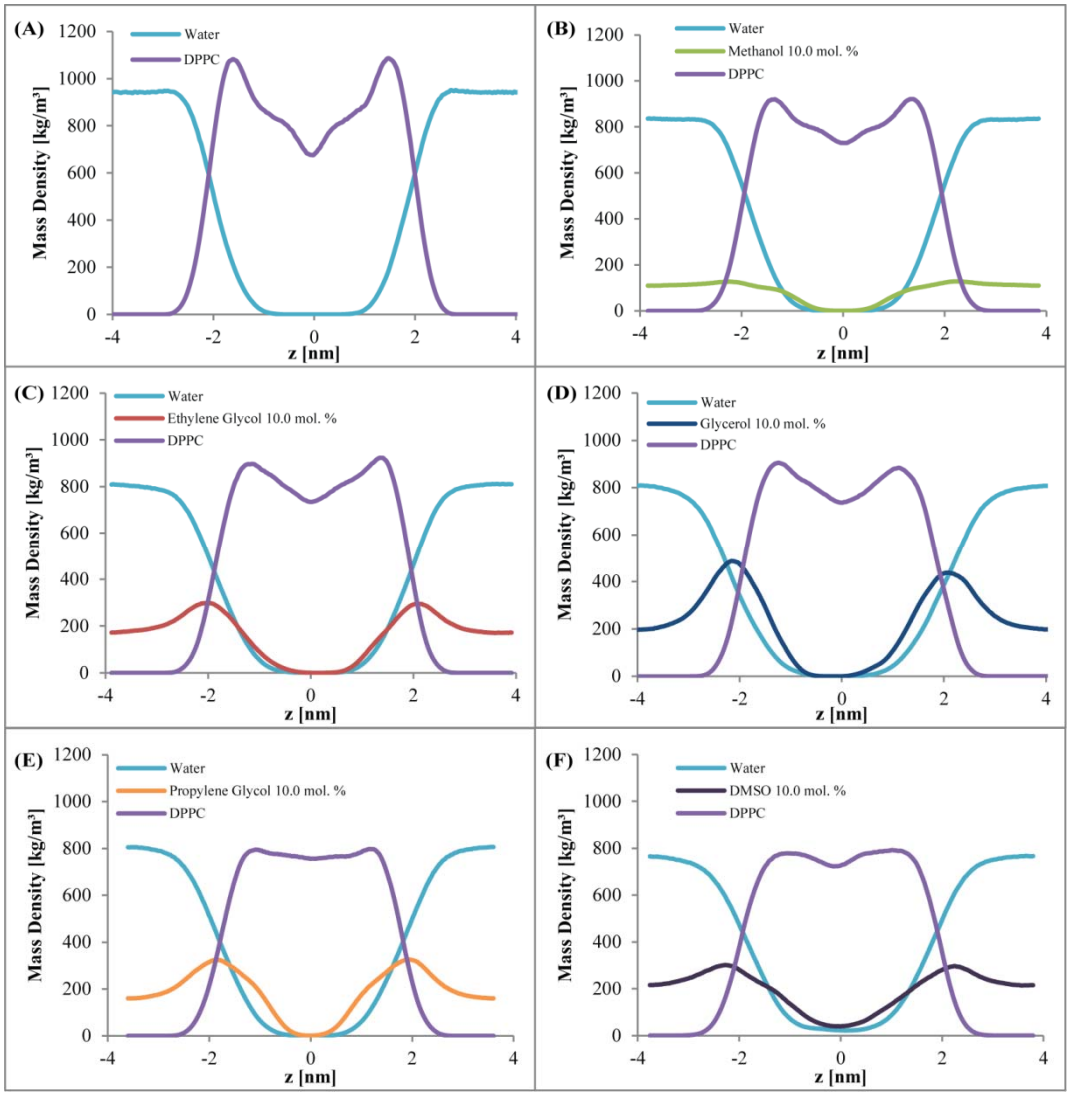

Fig. 6. MDPs perpendicular to the plane of the DPPC membranes without cryosolvent, and in the presence of (*A*) no cryosolvent, and (*B*) MET, (*C*) EG (*D*) GLY, (*E*) PG, and (*F*) DMSO, at 10.0 mol. %.

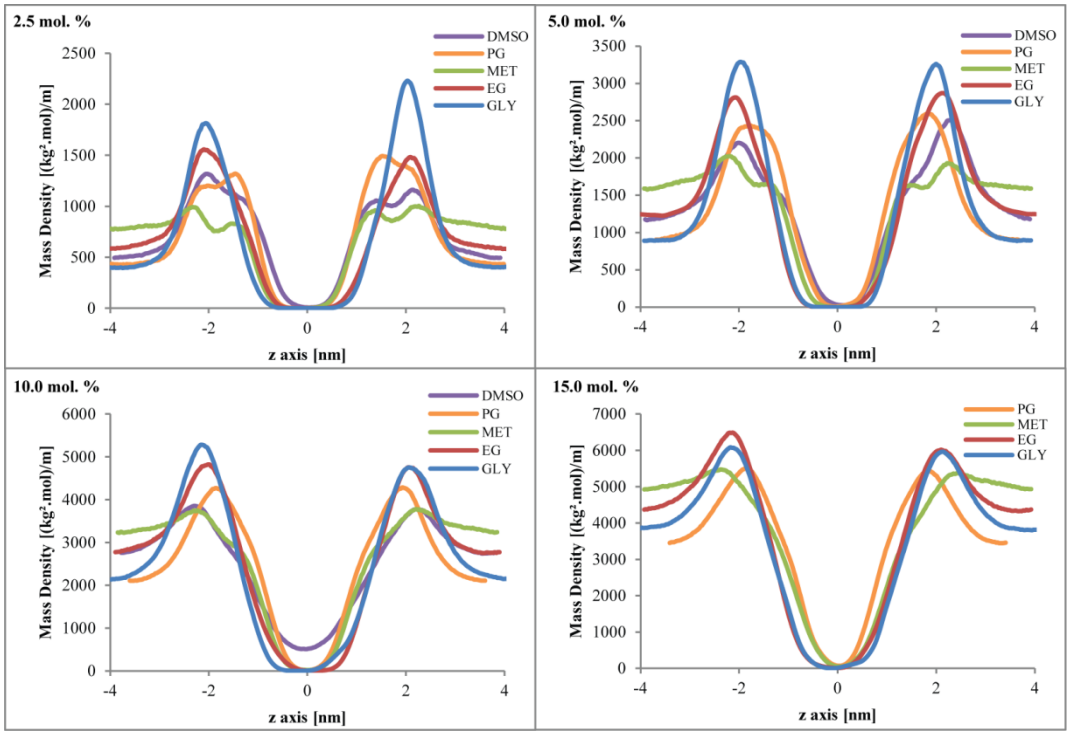

Fig. 7. The number density profiles for each concentration of cryosolvent in the DPPC bilayer system.

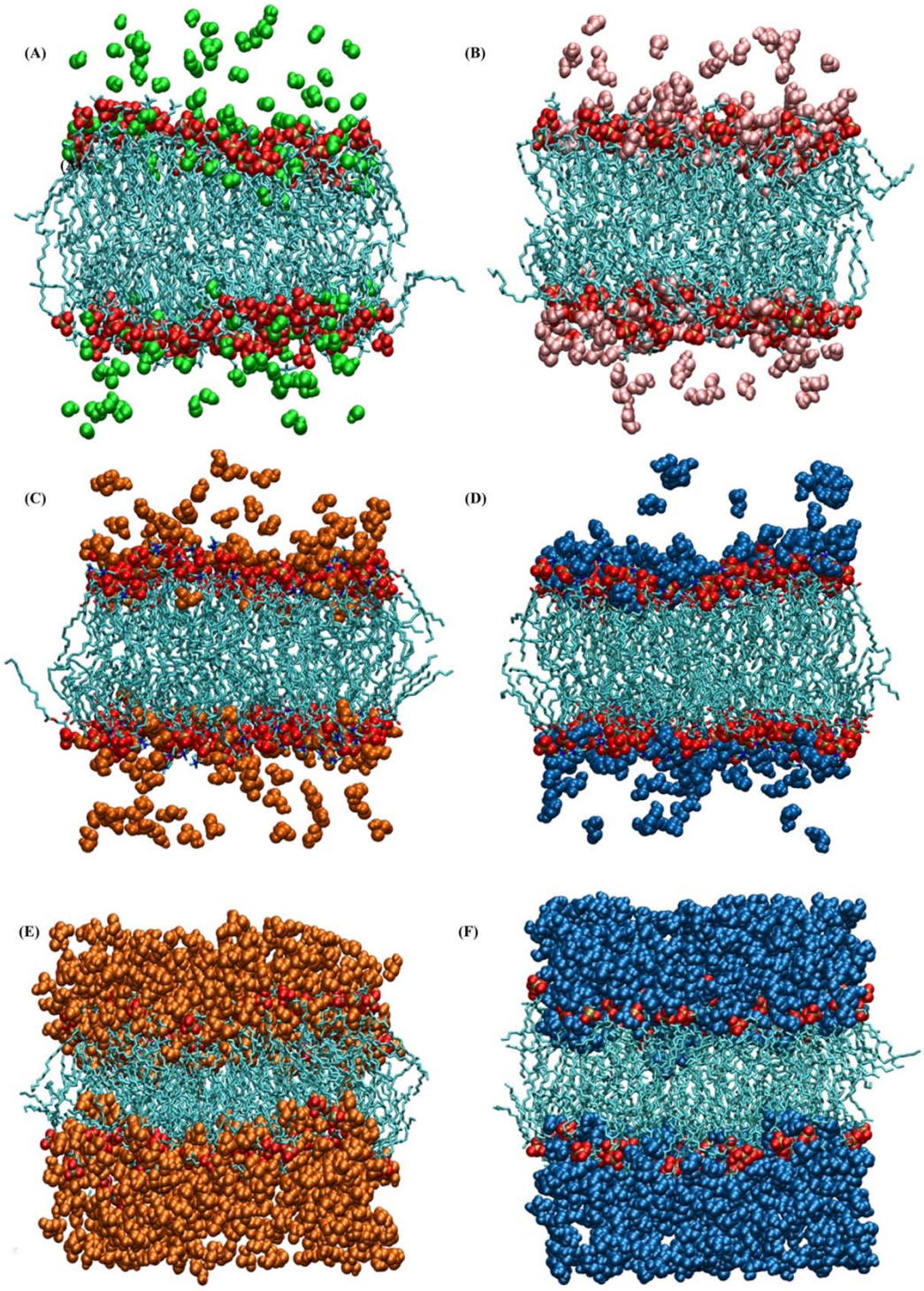

Fig. 8. Configuration snapshots taken from simulations of a DPPC bilayer in the presence of 2.5 mol. % *(A)* MET, *(B)* EG, *(C)* PG, *(D)* GLY, and 15.0 mol. % *(E)* PG, and *(F)* GLY. MET, EG, PG and GLY are coloured green, pink, orange and blue, respectively. All phospholipid phosphate groups are coloured red, and the phospholipid tail groups are coloured cyan.

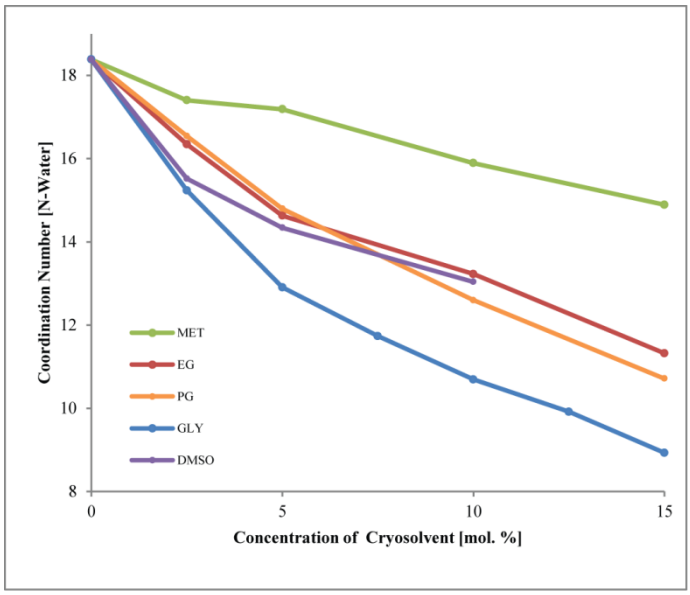

Fig. 9. Water coordination numbers for nitrogen atoms in the DPPC head groups as a function of molar concentration of each cryosolvent.

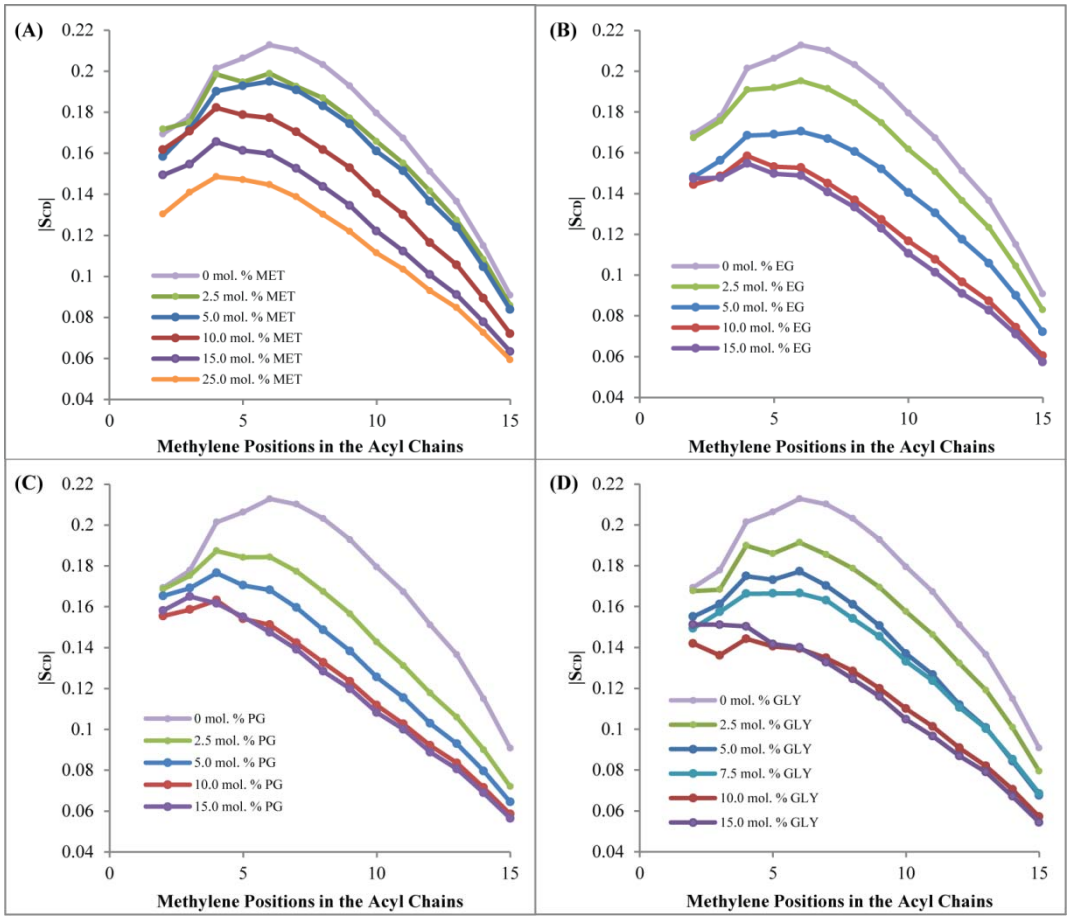

Fig. 10. Deuterium order parameters for *sn*-2 chains for DPPC bilayer systems in the presence of *(A)* MET, *(B)* EG, *(C)* PG, and *(D)* GLY across a range of concentrations.

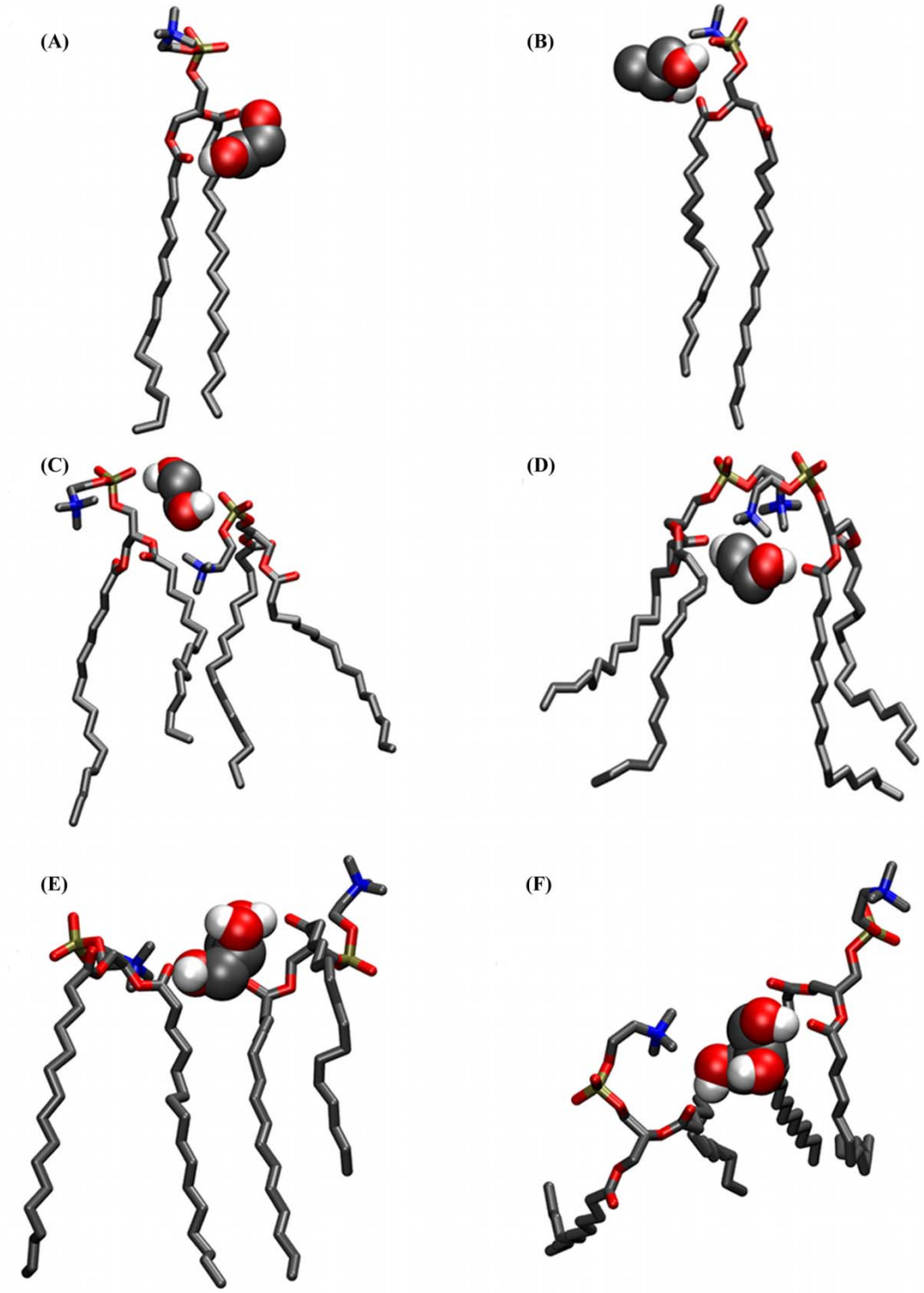

Fig. 11. Snapshots taken from the y-direction of *(A)* an EG molecule interacting with the two glycerol moieties of one DPPC phospholipid, *(B)* a PG molecule interacting with one glycerol moiety and one phosphate moiety of one DPPC phospholipid, *(C)* cross-linking of two DPPC phospholipids at their respective phosphate groups *via* a PG molecule, *(D)* cross-linking of two DPPC phospholipids at their glycerol groups *via* an EG molecule, and *(E)* cross-linking of phospholipids *via* a GLY molecule interacting with two DPPC phospholipids. A snapshot of the same cross-linking event involving GLY taken from the z-direction is shown in *(F)*. All oxygen groups are coloured in red, hydrogen groups in white, carbon groups in grey, phosphate groups in gold, and nitrogen groups in blue.

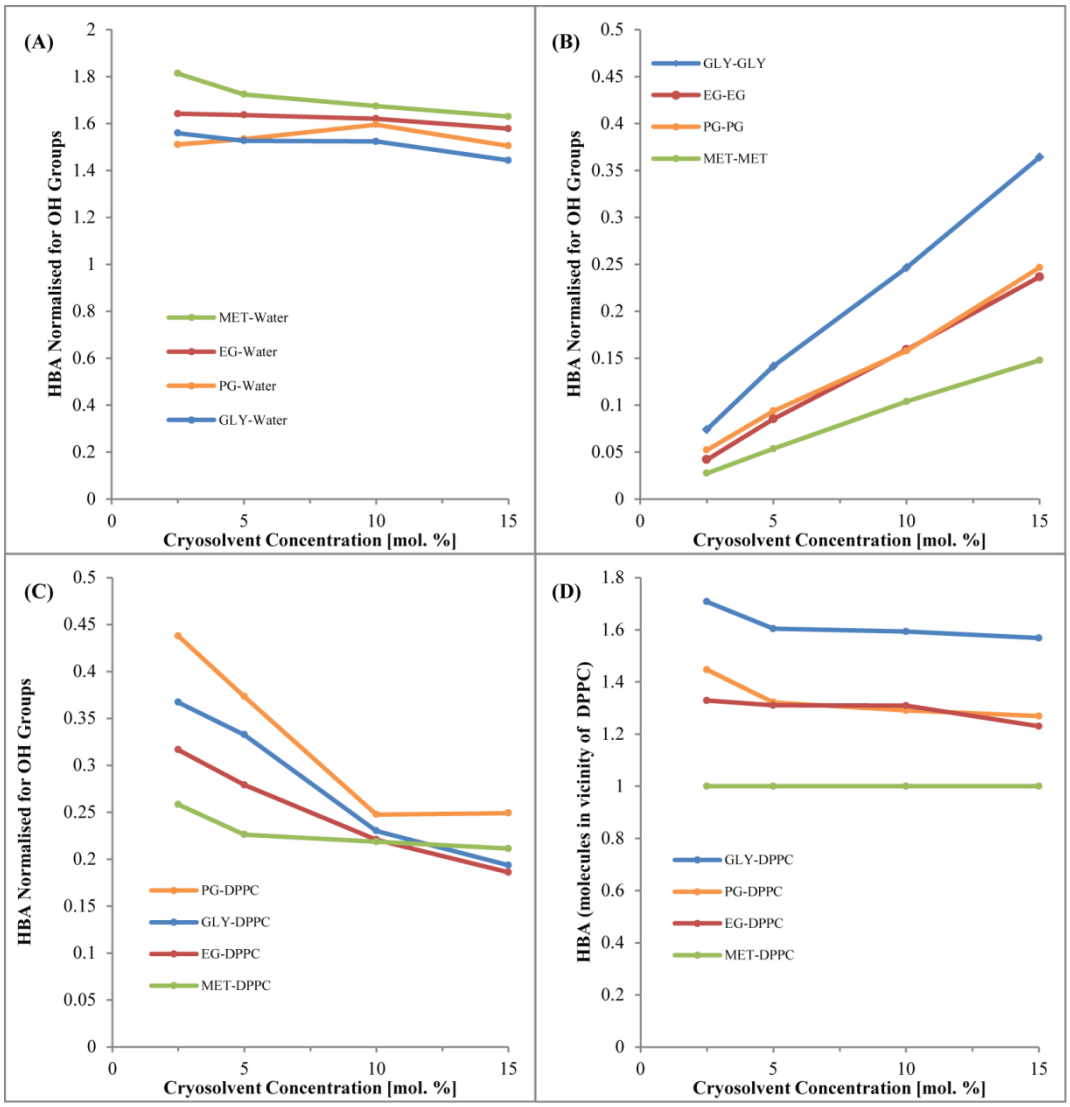

Fig. 12. Hydrogen bonding affinity (HBA) of the cryosolvents to *(A)* water, *(B)* cryosolvent molecules, *(C)* the DPPC lipid bilayer, normalised for cryosolvent hydrogen-bond donor groups, and (*D)* in the vicinity of the bilayer to the DPPC headgroups.

Table 1. DPPC membrane thickness (measured as the average distance between phosphate headgroups between the two leaflets) and APL as a measure of cryosolvent concentration.

Cryosolvent	Concentration [mol.%]	$d_{membrane}$ [nm]	APL [nm^2]	% APL increase
None	0	3.70 ± 0.03	0.622 ± 0.009	0
MET	2.5	3.65 ± 0.05	0.649 ± 0.011	7.1
	5.0	3.56 ± 0.05	0.676 ± 0.011	8.6
	10.0	3.43 ± 0.06	0.731 ± 0.017	17.5
	15.0	3.30 ± 0.06	0.785 ± 0.015	26.2
	25.0	3.09 ± 0.06	0.843 ± 0.019	35.5
EG	2.5	3.60 ± 0.06	0.660 ± 0.013	6.1
	5.0	3.42 ± 0.06	0.702 ± 0.013	12.9
	10.0	3.31 ± 0.05	0.745 ± 0.016	19.8
	15.0	3.23 ± 0.05	0.777 ± 0.017	24.9
PG	2.5	3.47 ± 0.05	0.705 ± 0.013	13.3
	5.0	3.32 ± 0.06	0.756 ± 0.016	21.5
	10.0	3.12 ± 0.05	0.846 ± 0.015	36.0
	15.0	3.02 ± 0.04	0.902 ± 0.015	45.0
GLY	2.5	3.57 ± 0.07	0.664 ± 0.014	6.8
	5.0	3.44 ± 0.04	0.707 ± 0.011	13.7
	7.5	3.42 ± 0.07	0.719 ± 0.017	15.6
	10.0	3.28 ± 0.05	0.759 ± 0.011	22.0
	12.5	3.25 ± 0.04	0.772 ± 0.017	24.1
	15.0	3.27 ± 0.05	0.774 ± 0.013	24.4
DMSO	2.5	3.54 ± 0.07	0.702 ± 0.013	12.8
	5.0	3.49 ± 0.07	0.772 ± 0.014	16.1

10.0	3.55 ± 0.09	0.850 ± 0.017	36.6

Table 2. Bulk-to-peak height ratios of the cryosolvents MET, EG, PG and GLY in DPPC bilayer systems.

Cryosolvent	**Concentration [mol. %]**			
	2.5	**5.0**	**10.0**	**15.0**
MET	1.21	1.21	1.14	1.11
EG	2.63	2.28	1.76	1.44
PG	3.29	2.78	2.03	1.58
GLY	5.94	3.55	2.34	1.65
DMSO	2.51	2.01	1.39	-

Table 3. Water coordination numbers for carbonyl oxygen of the DPPC glycerol head group as a function of mol. percentage of each cryosolvent.

Cryosolvent	**Concentration [mol. %]**			
	0	**2.5**	**5**	**10**
MET	1.8 ± 0.1	1.6 ± 0.1	1.5 ± 0.1	1.3 ± 0.1
EG	1.8 ± 0.1	1.4 ± 0.1	1.3 ± 0.1	1.1 ± 0.1
PG	1.8 ± 0.1	1.4 ± 0.1	1.2 ± 0.1	1.0 ± 0.1
GLY	1.8 ± 0.1	1.3 ± 0.1	1.0 ± 0.1	0.8 ± 0.1
DMSO	1.8 ± 0.1	1.7 ± 0.1	1.7 ± 0.1	1.6 ± 0.1

Table 4. Average total number of hydrogen bonds between the cryosolvents (MET, EG, GLY and DMSO) and water with the glycerol and phosphate head groups of a DPPC bilayer, calculated for each 60 ns simulation of a DPPC bilayer in the absence or presence of different cryosolvents.

Cryosolvent	**Cryosolvent Concentration [mol. %]**					
	0	**2.5**	**5**	**10**	**15**	**25**
MET						
MET - Glycerol	0	22 ± 3	39 ± 6	65 ± 14	84 ± 7	114 ± 8
MET - Phosphate	0	17 ± 4	33 ± 5	61 ± 14	88 ± 8	125 ± 9
Water-Glycerol	301 ± 10	296 ± 17	271 ± 14	269 ± 9	239 ± 10	214 ± 10
Water-Phosphate	409 ± 11	409 ± 16	392 ± 8	360 ± 8	340 ± 10	259 ± 9
EG						
EG - Glycerol	0	42 ± 5	71 ± 6	102 ± 8	126 ± 8	
EG - Phosphate	0	50 ± 6	90 ± 8	142 ± 11	173 ± 9	
Water - Glycerol	301 ± 10	275 ± 12	224 ± 18	241 ± 18	209 ± 19	
Water - Phosphate	409 ± 11	343 ± 15	318 ± 13	282 ± 11	218 ± 11	
PG						
PG - Glycerol	0	61 ± 6	92 ± 8	112 ± 10	164 ± 10	
PG - Phosphate	0	54 ± 6	104 ± 8	133 ± 11	197 ± 10	
Water - Glycerol	301 ± 10	253 ± 16	256 ± 12	191 ± 11	165 ± 12	
Water - Phosphate	409 ± 11	356 ± 19	311 ± 10	256 ± 11	234 ± 10	
GLY						
GLY - Glycerol	0	60 ± 6	108 ± 7	140 ± 7	162 ± 10	
GLY - Phosphate	0	89 ± 9	144 ± 8	208 ± 10	232 ± 9	
Water - Glycerol	301 ± 10	275 ± 12	224 ± 18	241 ± 11	209 ± 17	
Water - Phosphate	409 ± 11	343 ± 18	318 ± 7	282 ± 13	218 ± 10	
DMSO						
-Water-Glycerol	301 ± 10	301 ± 11	292 ± 12	290 ± 10		
- Water-Phosphate	409 ± 11	391 ± 11	374 ± 12	353 ± 13		

Table 5. The average number of hydrogen bonds that a cryosolvent molecule hydrogen bonded to the DPPC bilayer forms with the glycerol and phosphate groups, calculated and averaged from 10 snapshots across a 60 ns period.

Cryosolvent	**Cryosolvent Concentration [mol. %]**			
	2.5	**5**	**10**	**15**
EG				
EG - Glycerol	1.34± 0.2	1.64 ± 0.1	1.50 ± 0.1	1.57 ± 0.1
EG - Phosphate	1.42± 0.2	1.03 ± 0.1	1.09 ± 0.1	1.01 ± 0.1
PG				
PG - Glycerol	1.32± 0.1	1.65 ± 0.1	1.54 ± 0.1	1.57 ± 0.1
PG - Phosphate	1.40 ± 0.1	1.04 ± 0.1	1.11 ± 0.1	1.02 ± 0.1
GLY				
GLY - Glycerol	2.65 ± 0.2	2.58 ± 0.1	2.37 ± 0.1	1.89 ± 0.1
GLY - Phosphate	1.08 ± 0.1	1.04 ± 0.1	1.05 ± 0.1	1.24 ± 0.2

Table 6. The number of double and triple hydrogen bonds formed between cryosolvent molecules and the DPPC molecules for ethylene glycol, propylene glycol and glycerol.

Cryosolvent	**Concentration [mol. %]**			
	2.5	**5**	**10**	**15**
EG				
Dual H-bonding Molecules (DBM)	23 ± 1	34 ± 2	57 ± 5	59 ± 2
Total EG Molecules	64 ± 3	107 ± 11	187 ± 9	235 ± 7
Ratio (DBM :Total)	0.36	0.31	0.31	0.25
PG				
Dual H-bonding Molecules (DBM)	32 ± 3	41 ± 3	65 ± 3	73 ± 4
Total PG Molecules	85 ± 6	137 ± 4	232 ± 4	284 ± 6
Ratio (DBM :Total)	0.38	0.30	0.28	0.26
GLY				
Dual H-bonding Molecules (DBM)	34 ± 1	56 ± 3	79 ± 2	84 ± 1
Triple H-bonding Molecules (TBM)	14 ± 1	21 ± 4	26 ± 1	26 ± 4
Total Multi-H-bonding Molecules (MBM)	48 ± 2	77 ± 7	105 ± 3	109 ± 5
Total GLY Molecules	89 ± 1	154 ± 1	226 ± 3	254 ± 1
Ratio (DBM :Total)	0.38	0.37	0.35	0.33
Ratio (TBM : Total)	0.16	0.14	0.12	0.10
Ratio (MBM :Total)	0.53	0.50	0.47	0.43

Supporting Information

Fig. S1. MDPs perpendicular to the plane of the DPPC membranes in the presence of (*A*) MET, (*B*) EG (*C*) GLY, and (*D*) PG at 15.0 mol. %.